Northwest Flow Snow Aspects of Hurricane Sandy

STEVE KEIGHTON,* DOUGLAS K. MILLER,+ DAVID HOTZ,# PATRICK D. MOORE,@ L. BAKER PERRY,& LAURENCE G. LEE,@,++ AND DANIEL T. MARTIN**

* *National Weather Service, Blacksburg, Virginia*
+ *University of North Carolina at Asheville, Asheville, North Carolina*
# *National Weather Service, Morristown, Tennessee*
@ *National Weather Service, Greenville–Spartanburg, South Carolina*
& *Appalachian State University, Boone, North Carolina*
** *GBE Fund, Inc., Calgary, Alberta, Canada*

(Manuscript received 28 May 2015, in final form 6 November 2015)

ABSTRACT

In late October 2012, Hurricane Sandy tracked along the eastern U.S. coastline and made landfall over New Jersey after turning sharply northwest and becoming posttropical while interacting with a complex upper-level low pressure system that had brought cold air into the Appalachian region. The cold air, intensified by the extreme low pressure tracking just north of the region, combined with deep moisture and topographically enhanced ascent to produce an unusual and high-impact early season northwest flow snow (NWFS) that has no analog in recent history. This paper investigates the importance of the synoptic-scale pattern, forcing mechanisms, moisture characteristics (content, depth, and likely sources), and low-level winds, as well as the evolution of some of these features compared to more typical NWFS events in the southern Appalachian Mountains. Several other aspects of the Sandy snowfall event are investigated, including low-level stability and mountain wave formation as manifested in vertical profiles and radar observations. The importance to operational forecasters of recognizing and understanding these factors and differences from more common NWFS events is also discussed.

1. Introduction

Major impacts to the United States from Hurricane Sandy went beyond damage from storm surge flooding and high winds (Blake et al. 2013). As remnants of Sandy tracked northwestward and inland over the mid-Atlantic region of the United States on 29–31 October 2012 (Fig. 1) while interacting with a strong midlatitude upper-level trough digging southeastward from Canada, historic early season snowfall with blizzard conditions occurred over much of the southern Appalachian Mountains (SAMs). Northwest winds associated with the strong pressure gradient on the periphery of Sandy intensified the cold-air advection and enhanced orographic lift on the western slopes of the mountain ridges, leading to a changeover from rain to snow and increasing precipitation rates from the strengthening upward motion.

Partly due to the intensity as well as the longevity of the event, most locations along the western slopes of the SAMs received 20–30 cm of snowfall on 29–31 October 2012, with isolated elevations above 1200 m receiving 70–80 cm (Fig. 2). October monthly snowfall records were broken (many by a large margin) at almost two dozen official climate stations across the SAMs. In addition to the extreme snowfall, persistent strong winds and frequent gusts over 20 m s^{-1} were common across the SAMs, with isolated peak gusts over 30 m s^{-1} and one at Grandfather Mountain, North Carolina (1609 m), exceeding 45 m s^{-1}. This resulted in significant blowing and drifting of the snow, despite its relatively wet and heavy characteristics.

Significant impacts included numerous downed trees and power outages due to the combination of heavy snow and strong winds. West Virginia was the hardest hit, where power was out for up to 2 weeks in some

++ Retired.

Corresponding author address: Steve Keighton, National Weather Service, 1750 Forecast Dr., Blacksburg, VA 24060.
E-mail: stephen.keighton@noaa.gov

DOI: 10.1175/WAF-D-15-0069.1

© 2016 American Meteorological Society

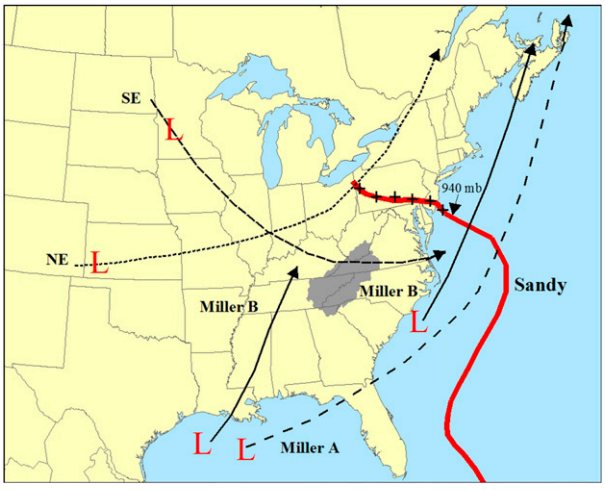

FIG. 1. Best track of Hurricane Sandy, including transition to an extratropical low pressure system (shown by plus signs) just before it moved inland [adapted from Blake et al. (2013)]. Superimposed are synoptic low pressure center tracks associated with common patterns leading to NWFS events in the SAMs. These are discussed further in section 2, and defined in Perry et al. (2013). The shaded area represents the original Perry et al. (2007) NWFS climatology study area. [Adapted from Perry et al. (2013).]

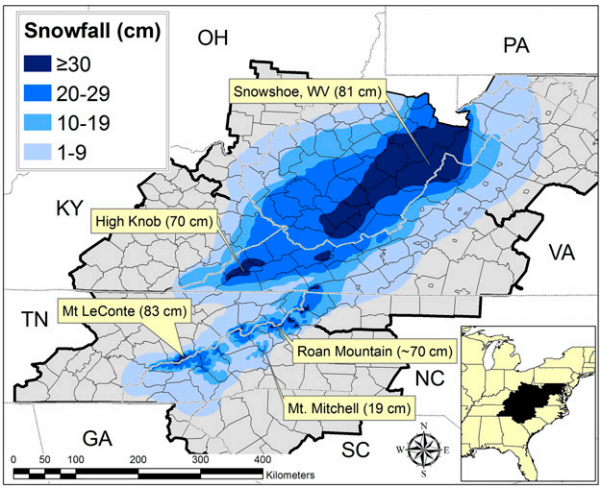

FIG. 2. Storm total snow accumulation (cm) for the remnants of Sandy for 29–31 Oct 2012. [Adapted from Martin (2013).]

mountain locations, and 50 homes were damaged. Some roads were also closed during and after the storm as a result of snow drifts or downed trees and power lines. Over $10 million in damage was incurred within West Virginia alone, with 18 counties included in a Federal Disaster Declaration (FEMA 2012). Power outages were also reported across parts of southwest Virginia and eastern Kentucky.

To put Sandy's snowfall aspects into some historical context, only three snow events with origins from Atlantic basin tropical systems have been documented as impacting the United States. All three snow events were confined to New England: 1) one in October 1804 (Ludlum 1963); 2) another in February 1952, which was a brief unnamed tropical storm off the southeast U.S. coast,[1] and with only minor snow accumulations in northern New England (Department of Commerce 1952); and 3) Hurricane Ginny in late October 1963, which was associated with significant snow accumulations in Maine that caused two fatalities (Dunn 1964). It is worth noting while Ginny moved up the Atlantic coast and cold air was pulled in behind the circulation that trace amounts of snow were reported at Grandfather Mountain, North Carolina (1616 m), and thus one case where at least some light snowfall in the SAMs may have been indirectly associated with a tropical system.

The climatology, characteristics, evolutions, favored patterns, and other details of snowfall in the SAMs are heavily influenced by low-level northwest flow (a very

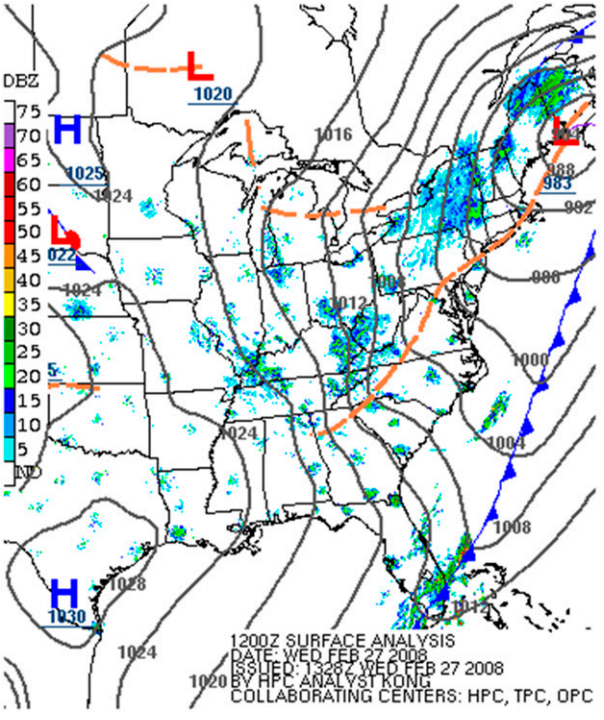

FIG. 3. Surface analysis (MSLP, in dark gray, analyzed frontal positions, and radar mosaic) during a typical NWFS event in the SAMs (1200 UTC 27 Feb 2008). [Image adapted from the NCEP Weather Prediction Center online (http://www.wpc.ncep.noaa.gov/archives/web_pages/sfc/sfc_archive.php).]

[1] NHC HURDAT update documentation is available online (http://www.aoml.noaa.gov/hrd/hurdat/metadata_master.html#1952_1).

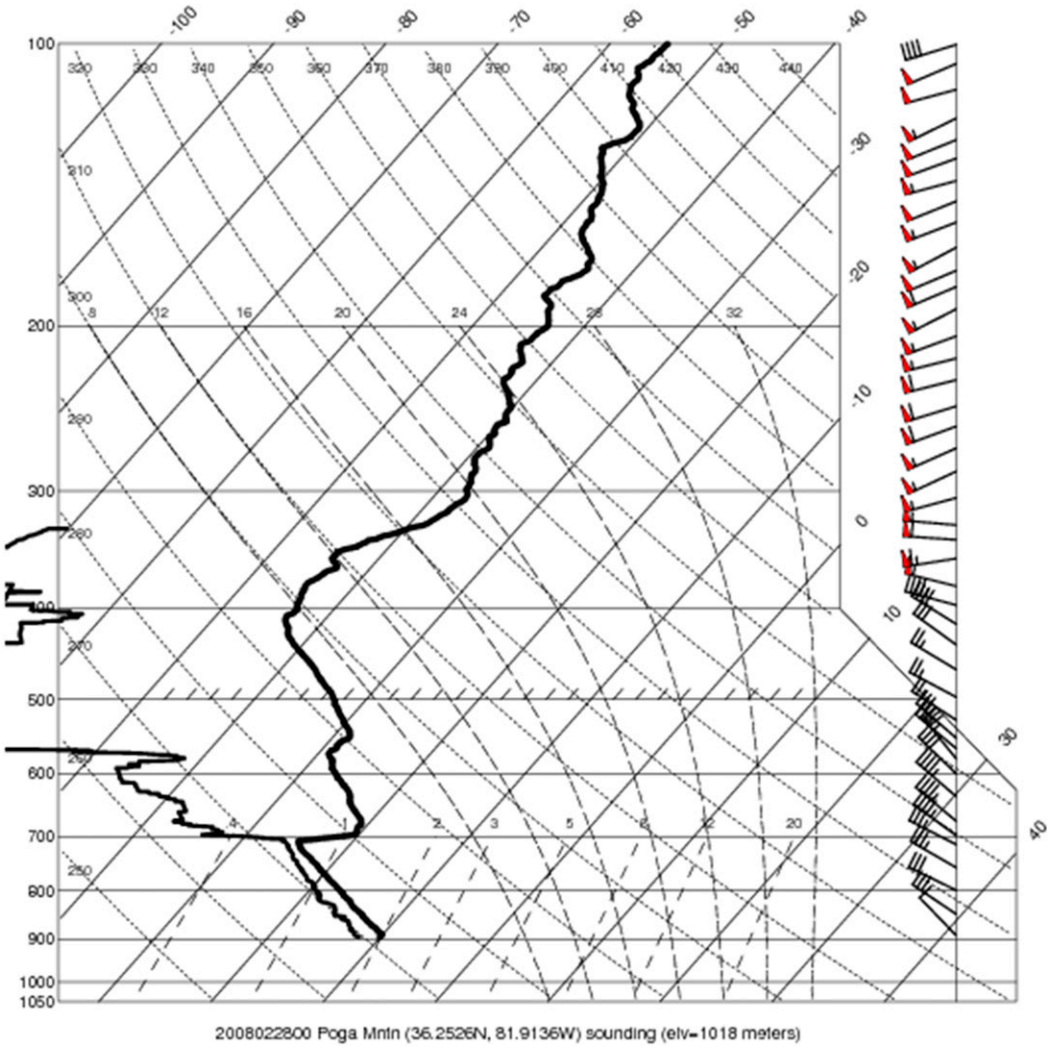

FIG. 4. Sounding launched from Poga Mountain in northwest NC (this location can be seen in Fig. 5 as the point labeled B) during an NWFS event at 0000 UTC 28 Feb 2008.

common, and in many locations dominant, low-level flow direction for snowfall in the SAMs), and have been studied closely over a number of years recently by a collaborative group of scientists from the operational and academic community (e.g., Keighton et al. 2009). With Sandy, the northwest flow snow (NWFS) aspects are observed to be unique on a number of levels compared to more typical NWFS events in the SAMs, including the tropical origin and likely sources of moisture, moisture depth and content, pressure gradient and associated low-level wind speeds, and strength of mountain wave development. Yet at the same time there are some similarities in terms of favored locations (overall snowfall pattern), persistent low-level northwest flow through the duration of the event, and shallow surface-based instability. Some NWFS events do evolve from synoptic-scale coastal storm systems with an initial period of deeper moisture and deep large-scale ascent over the SAMs on the northwest side the surface low (often with east or northeasterly low-level winds during the heaviest snowfall) before transitioning to a typical NWFS scenario with shallow moisture and dominant orographic influences on the back side of the storm. The variety of evolutions resulting in NWFS events will be discussed in more detail in section 2.

Given that the Sandy snowfall totals (and especially the liquid equivalent measurements) were more extreme than with typical NWFS events, this study investigates specifically how and why the synoptic evolution, forcing mechanisms, moisture characteristics and sources, wind, and cloud-layer temperatures were unique with Sandy compared to more typical NWFS

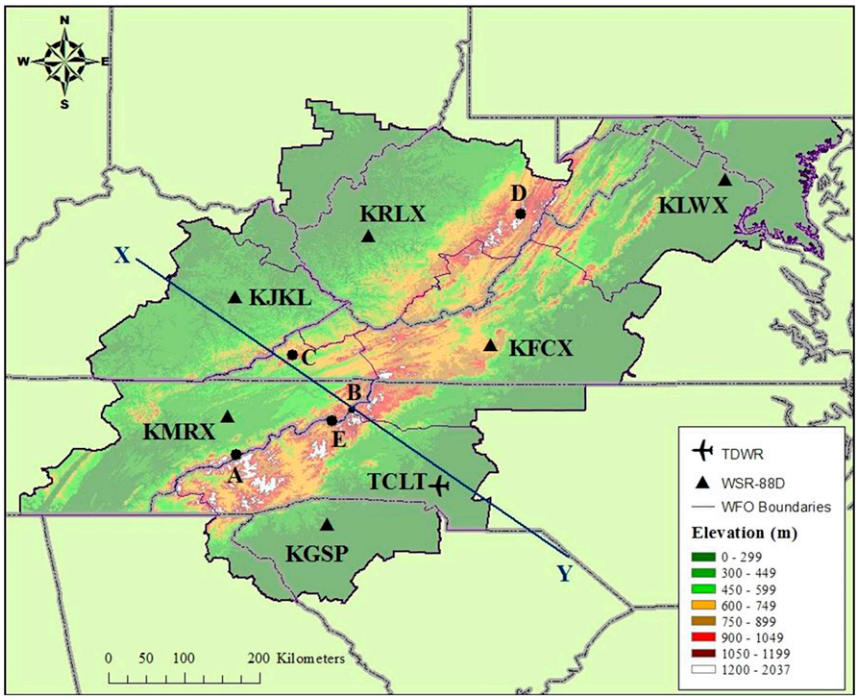

FIG. 5. Domain of the NWFS study area, with boundaries of NWS forecast office areas of responsibility, terrain background image, Doppler radar locations, a cross-section position (X–Y) referred to in sections 4 and 5, and labels for five locations primarily referred to in section 4. The lettered labels represent the following locations: A, Mount LeConte (elevation 2010 m); B, Poga Mountain (elevation 1018 m); C, High Knob (elevation 1287 m); D, Snowshoe (elevation 1436 m); and E, Roan Mountain (elevation 1916 m).

events in the SAMs. An identification and understanding of the unique NWFS aspects of Sandy will help forecasters to better anticipate impacts from future potentially extreme NWFS events, especially those that may have tropical origins.

Section 2 of this paper provides a brief summary of recent studies and collaborative efforts to better understand NWFS events in the SAMs, including the climatology, impacts, spatial and temporal variation of snowfall, and associated synoptic patterns; section 3 describes the synoptic evolution of Sandy during the snowfall phase and also examines the forcing mechanisms primarily responsible for most of the snowfall; section 4 focuses mainly on the moisture characteristics, using trajectory analysis and comparisons with NWFS climatology; section 5 describes some unique radar observations not previously observed with more typical NWFS events and discusses their possible significance; and section 6 offers concluding thoughts and areas where future study is needed.

2. Review of NWFS in the SAMs

NWFS in the SAMs occurs during periods of moist upslope flow in association with northwest low-level winds, and can often result in significant but highly variable snowfall accumulations across the region, favored on northwest-facing slopes. These events frequently occur in the absence of synoptic-scale, deep vertical motion, as documented in initial climatological studies (Perry and Konrad 2006; Perry et al. 2007), and can either be very short lived or last for 2–3 days. Cold temperatures and strong winds, causing blowing and drifting of dry snow, often exacerbate the impact of snowfall on the rising permanent and especially transient population across parts of this region, especially tourism in far western North Carolina (Strom and Kerstein 2015).

A majority of NWFS events are postfrontal, with shallow moisture (<3.0 km MSL) and cold-air advection; the air in the shallow cloud layer becomes cold enough for dendritic ice crystal growth [from −12° to −18°C; Libbrecht (2005)]. Moisture sources most frequently come from the Great Lakes or even from moist ground more immediately upstream based on trajectory analysis and numerical modeling studies (Perry et al. 2007; Holloway 2007; Miller 2012). However, in the early stages of some NWFS events the moisture may begin as ''wrap around'' on the west side

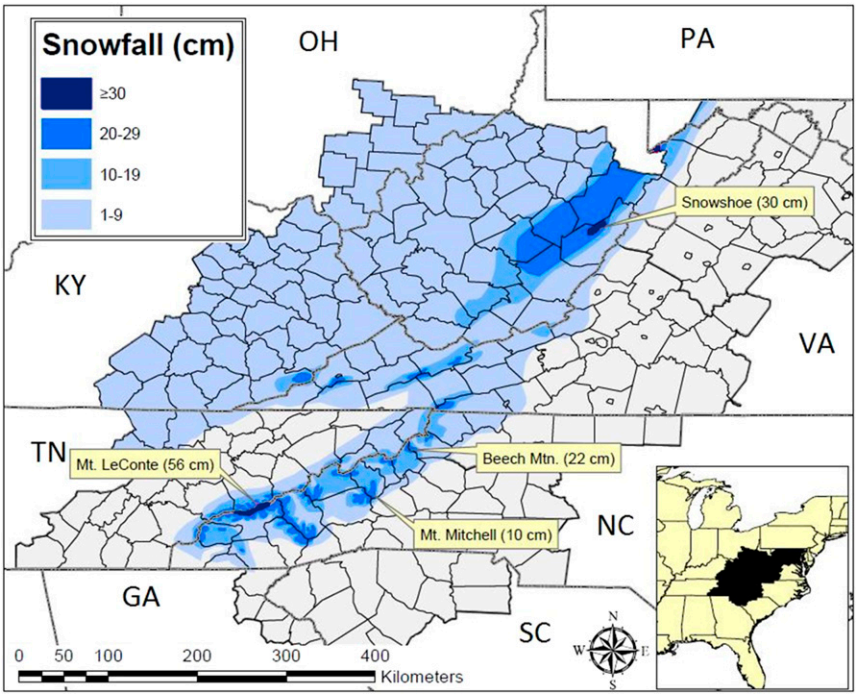

FIG. 6. Storm total snowfall (cm) for a typical NWFS event (27–28 Feb 2008). Inset shows this region within the larger context of the eastern United States.

of a synoptic low pressure system moving up the East Coast and, thus, could have an Atlantic or Gulf of Mexico origin.

A relatively deep and unstable boundary layer is usually also present, similar to well-documented traditional lake-effect events (Schmidlin 1992; Niziol et al. 1995). The surface pattern during the time of a typical NWFS event (e.g., 27 February 2008) shows a cold front well off the Atlantic coast and a strong pressure gradient over the Appalachians (Fig. 3). A sounding during the 27 February 2008 NWFS event (Fig. 4) exhibits the following characteristics typical of these events: an unstable, moist boundary layer below a subsidence inversion; the moist layer extending into the dendritic ice crystal growth region; and northwest flow in the surface-based unstable layer. Snow-to-liquid ratios (SLRs) vary considerably, even within a single NWFS event, from 10:1 or less to as high as 50:1, with an average of around 20:1 for all events with at least 1 in. of snowfall (Perry et al. 2008; Keighton and Lee 2013).

Given the dominance of orographic forcing, these events have a strong terrain signal, with northwest slopes being favored. Figure 5 shows the terrain within the SAMs region where these previous studies have been focused, as well as key locations that will be referenced throughout this paper, whereas Fig. 6 shows the snowfall distribution for a typical NWFS event (26–28 February 2008) for comparison.

The initial studies of NWFS events in the Appalachians (Perry 2006; Perry and Konrad 2006) focused on any snow event with a northwest wind component near ridgetop level (average elevation roughly 1500 m, so

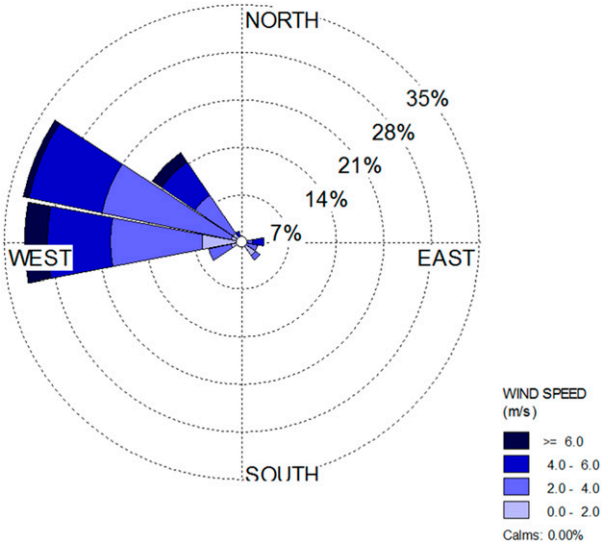

FIG. 7. Frequency of surface wind directions, and associated speeds, for all snow events at Poga Mountain from 2006 to 2012.

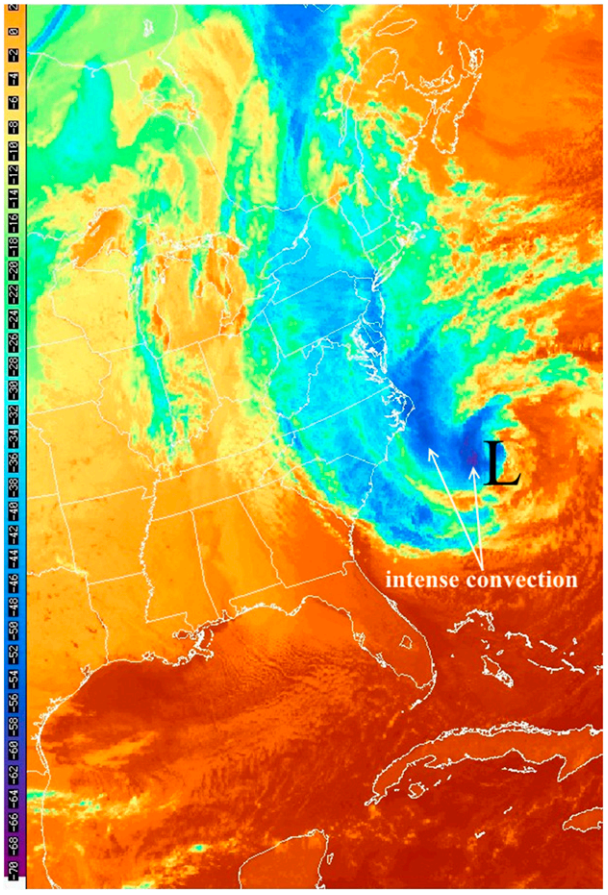

FIG. 8. *GOES-13* infrared satellite cloud-top temperature (°C) imagery valid 1200 UTC 28 Oct 2012. [Image courtesy of NCAR's online archive (http://locust.mmm.ucar.edu/imagearchive/, accessed on 17 Jun 2014).]

850 hPa was considered the most appropriate standard level), and found that in many areas along the western slopes of the SAMs as much as 30%–50% of the annual snowfall comes during northwest flow at this level. A more strict definition (e.g., Perry et al. 2007) includes the subset of these events where sinking motion is occurring at 700 hPa during event maturation (hour of heaviest snowfall), thereby focusing on NWFS events dominated by large-scale subsidence. Perry (2006) found that over a 50-yr period a majority (60%) of all NWFS events were accompanied by subsidence at 700 hPa at the time of event maturation. While some of the highest snowfall amounts in the SAMs come from events with low-level easterly or southeasterly winds at event maturation (i.e., low pressure systems moving up the southeast U.S. coast), these are relatively rare in terms of their frequency. Perry et al. (2013) showed that at Poga Mountain, North Carolina (1018 m, point B in Fig. 5), an extremely high percentage of all snow events (88%) was associated with west or northwest flow, with the remaining events (12%) associated with easterly flow (Fig. 7).

A synoptic classification scheme developed by Perry et al. (2010) for all snow events in the Great Smoky Mountain National Park (dominated by high elevations along the Tennessee–North Carolina border) was used later by Perry et al. (2013) to shed some light on the variety of patterns and evolutions leading to NWFS and their relative frequency of occurrence. Figure 1, in addition to including the track of Sandy, shows a schematic of a few of the more common cyclone tracks that can result in NWFS. Not shown however is the most frequent category, the "pure" upslope NWFS event, where no cyclone track (or associated large-scale lift) is directly associated with the period of snowfall. More discussion on these patterns and their frequency can be found in Perry at al. (2013). Of importance is that the Sandy track does not match any of the previously identified tracks and patterns, although it could be argued that it comes closest to the "Miller A" cyclogenesis pattern. It will be shown later that unlike many of the Miller A storms that produce the heaviest snowfall during low-level easterly flow, with Sandy a flow from northwest to west persisted from start to finish across the SAMs. Yet, there were many reasons why this was no typical NWFS event either, and these will be explored in the following sections. Additional details regarding much of the above-mentioned research and our current knowledge of NWFS in the SAMs are summarized in Keighton et al. (2009).

3. Evolution of Sandy's synoptic pattern, forcing mechanisms, and snow characteristics compared to a classic NWFS event

a. Synoptic overview and forcing

After Sandy reintensified on 27 October 2012, a critical period in Sandy's evolution occurred through 0000 UTC 29 October 2012, during which the track of the storm shifted toward the east coast of the United States. Galarneau et al. (2013) hypothesized that the "left turn" in Sandy's track was initiated by intense diabatic heating on the northwest flank of Sandy between 0000 UTC 28 October and 0000 UTC 29 October 2012 (Fig. 8). The associated upper-level divergent outflow, and associated production of anticyclonic vorticity, impeded the eastward progression of the overall 500-hPa level trough, allowing Sandy to track northward, rather than moving out to the open Atlantic Ocean.

At 0000 UTC 29 October (Fig. 9), a baroclinic zone was in place with the cold-air axis extending

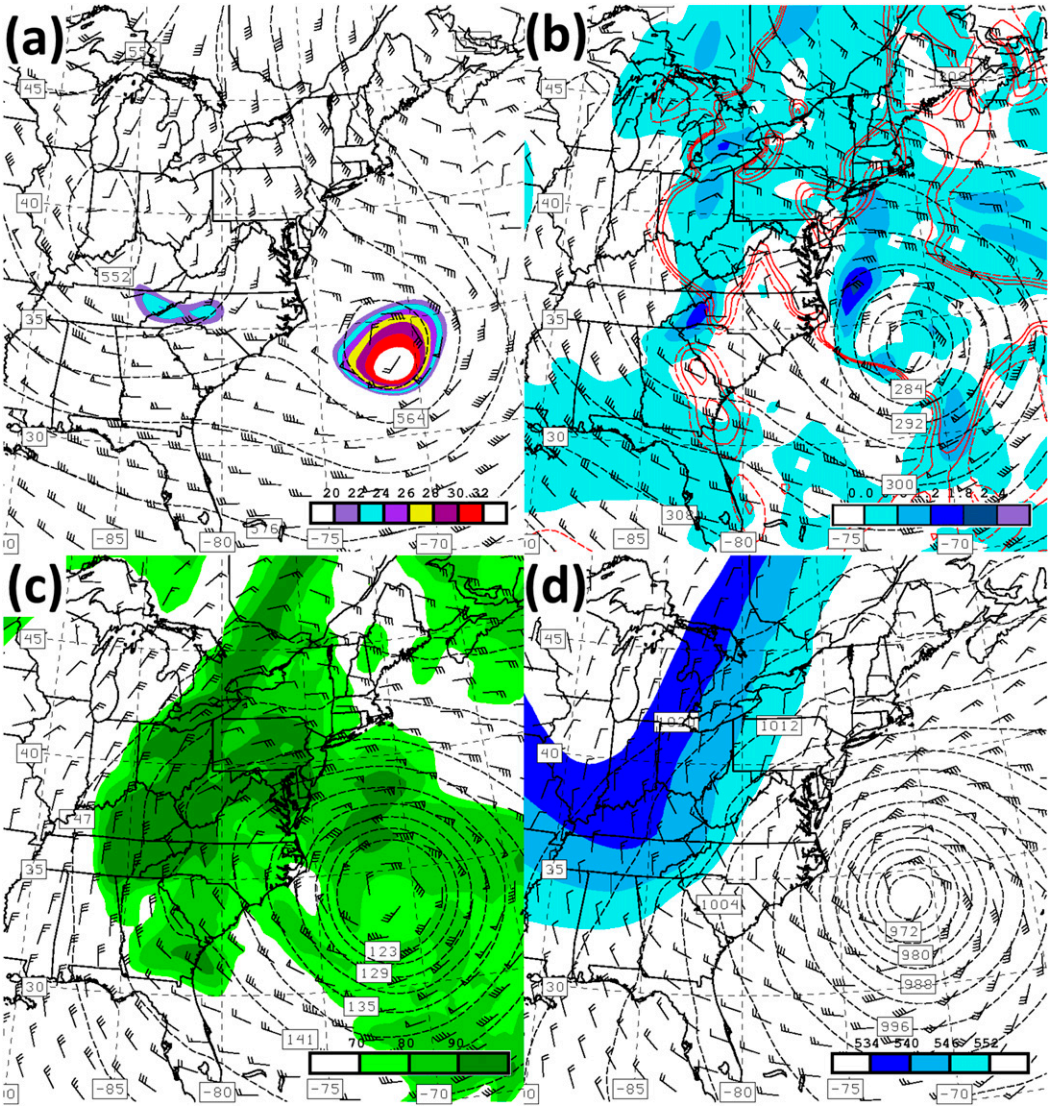

FIG. 9. NARR geopotential height (dm; dashed contours) and wind (kt, where 1 kt = 0.51 m s^{-1}; barbs) and (a) absolute vorticity ($\times 10^{-5}$ s^{-1}; shaded) at the 500-hPa level, (b) 750-hPa frontogenesis [shaded; K (100 km)$^{-1}$ (3 h)$^{-1}$] and 700-hPa upward motion (red contours; dashed shows the 0 contour, solid shows -0.5 and -1.0×10^{-3} hPa s^{-1}), (c) relative humidity (%; shaded) at the 850-hPa level, and (d) sea level pressure (hPa; dashed contours), 1000–500-hPa layer thickness (dm; shaded), and 10 m AGL winds valid at 0000 UTC 29 Oct 2012.

southeastward from Wisconsin (Fig. 9d), just west of the SAMs. The 500-hPa trough (Fig. 9a) attained a negative tilt as Sandy tracked northward. A broad region of rising motion occurred at the 700-hPa level near and to the northwest of the storm center (Fig. 9b), in response to the broad cyclonic vorticity advection occurring downstream of the 500-hPa trough, not driven locally by low-level frontogenesis (shading in Fig. 9b), which was weak and mainly centered over the terrain of western North Carolina. Abundant moisture was present on the upwind side of the SAMs as the wind circulated from the northwest at the 850-hPa level (Fig. 9c), although wind speeds and the associated pressure gradient were modest along the Tennessee–North Carolina border.

By 0000 UTC 30 October (Fig. 10), the remnants of Sandy, now categorized as an extratropical storm, linked with the 500-hPa-level polar trough (Fig. 10a) and moved toward the northwest, having made landfall along the New Jersey coast (Fig. 10d). Upward vertical motion at the 700-hPa level (Fig. 10b) was located primarily north of the storm center, exhibiting little

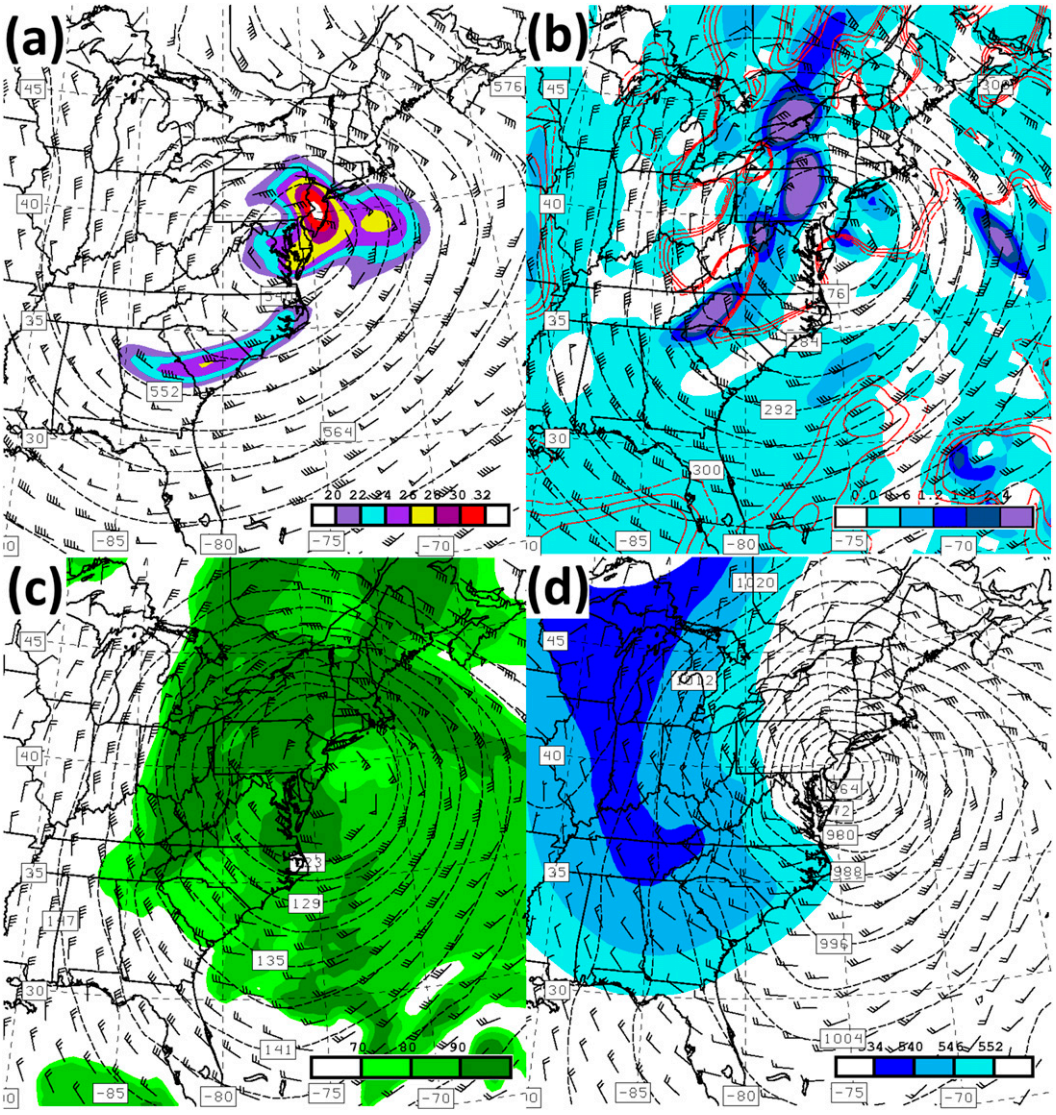

FIG. 10. As in Fig. 9, but at 0000 UTC 30 Oct 2012.

association with low-level frontogenesis regions over the SAMs. The storm deepened and, combined with its northwestward movement over the 24-h period, the pressure gradient strengthened over the SAMs and northwesterly wind speeds at the 850-hPa level increased (Fig. 10c). The cold-air mass drifted southward into eastern Tennessee (Fig. 10d), against the windward side of the SAMs, and narrowed starting at 0000 UTC 29 October.

The merger of the remnants of Sandy with the upper-level synoptic-scale wave was completed by 0000 UTC 31 October (Fig. 11) so that a massive vertically stacked low pressure system dominated the eastern United States from the surface (Fig. 11d) to the mid-troposphere (Fig. 11a). The storm center tracked far enough inland and toward the northwest that the intensity of the storm at low levels was greatly diminished (Figs. 11b–d) since 0000 UTC 30 October, with weaker northwesterly flow, disorganized 700-hPa-level upward vertical motion (generally west and north of the SAMs), and 850-hPa-level moisture moving away from the SAMs. The storm continued to fill and move northwestward away from the SAMs through 0000 UTC 1 November (not shown), but resulted in nearly a 72-h period of upslope flow for many locations. Despite this flow steadily weakening, the overall combination of upslope flow and abundant moisture resulted in a 50–65-h period of snowfall production for some locations.

The localized nature of the deepest snowfall accumulations (Fig. 2) suggests critical lift for precipitation

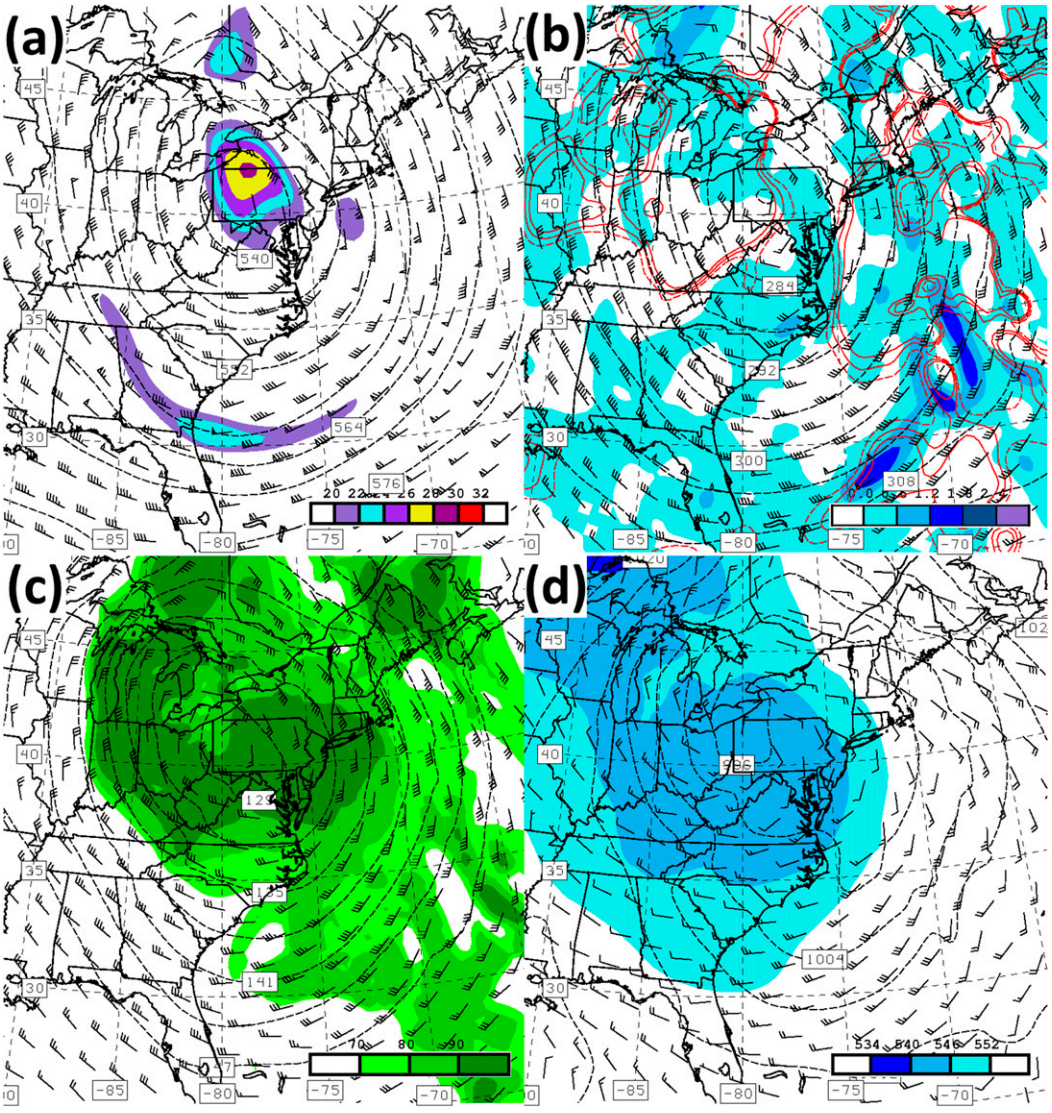

FIG. 11. As in Fig. 9, but at 0000 UTC 31 Oct 2012.

production was generated by upslope flow in the SAMs, rather than by regional synoptic-scale forcing mechanisms. Figures 9b, 10b, and 11b illustrate the general disconnect between 700-hPa vertical velocity and low-level (750-hPa level) frontogenesis, lending further support to the large accumulations with Sandy being forced by topography. Examination of cross-mountain-oriented vertical cross sections of vertical motion and frontogenesis at Poga Mountain (location B, with orientation labeled X–Y in Fig. 5) shown in Fig. 12 also points to the localized nature of the vertical motion and its associated forcing mechanisms. The extreme values of the fields in the 850–700-hPa layer, locked with topography at 0000 UTC 29 and 30 October (Figs. 12a,b), are indicative of the presence of a mountain wave (investigated further in section 5). Cross-mountain vertical sections of vertical motion and frontogenesis examined at Snowshoe, West Virginia (not shown), suggest that the lift at 0000 UTC 29 October was provided by regional synoptic-scale forcing, but clearly became terrain-driven soon thereafter.

b. *Snowfall characteristics during Sandy*

A unique perspective of Sandy was gleaned from the high-elevation site at Poga Mountain, where hourly precipitation and wind were measured. After initially beginning as light rain, precipitation quickly changed to snow by 0200 UTC 29 October in the wake of sufficient cold-air advection from the system. Snowfall remained constant through about 1800 UTC 30 October, when it

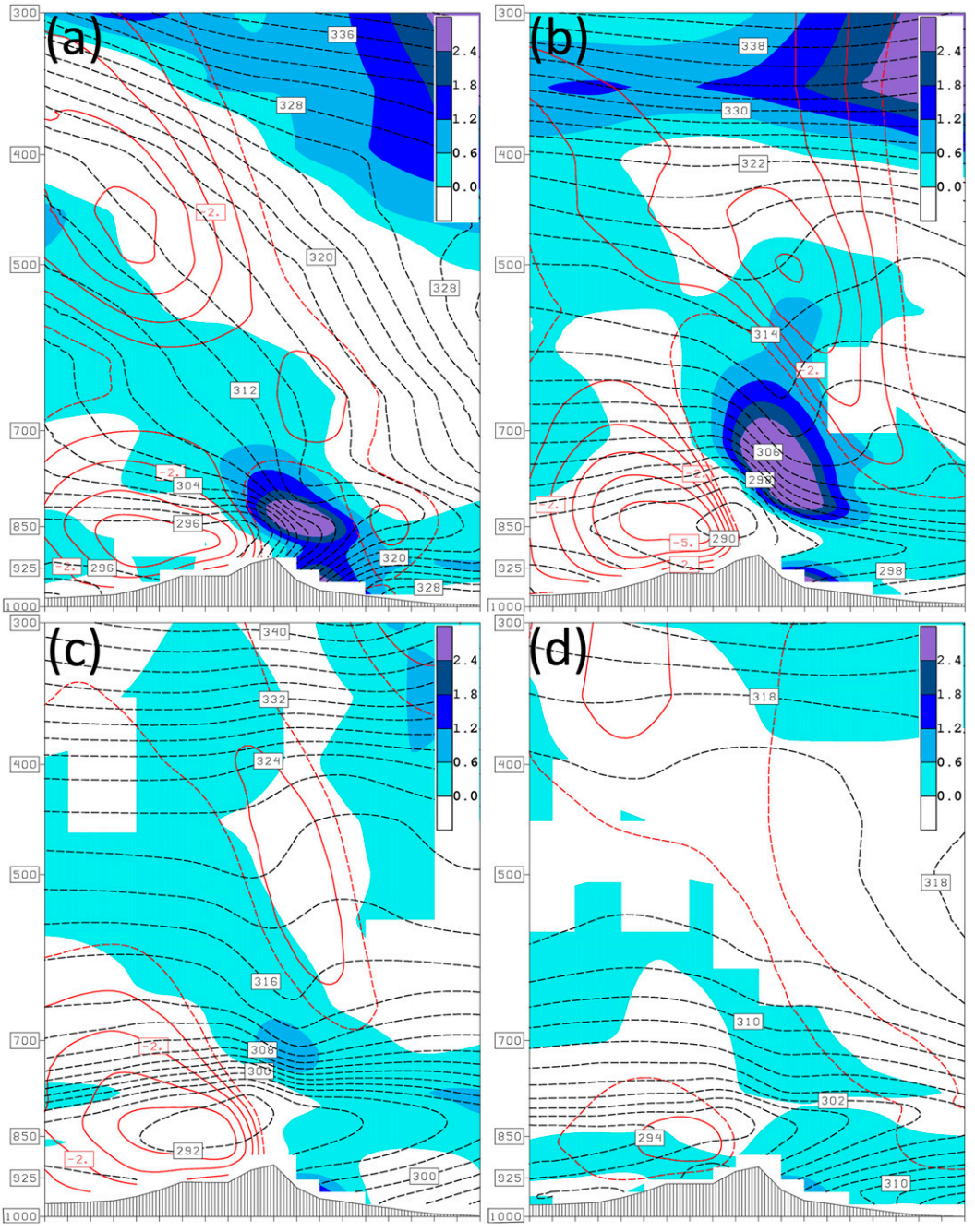

FIG. 12. Vertical cross sections from the NARR dataset for the line segment X–Y in Fig. 5 of frontogenesis [shaded; K (100 km)$^{-1}$ (3 h)$^{-1}$], with upward motion in red [plotted every 1×10^{-3} hPa s^{-1} from 0 (dashed) to -8×10^{-3} hPa s^{-1}], and saturation equivalent potential temperature (dashed black contours in 2-K intervals) for the following times: (a) 0000 UTC 29 Oct, (b) 0000 UTC 30 Oct, (c) 0000 UTC 31 Oct, and (d) 0000 UTC 1 Nov 2012.

then became intermittent through 1500 UTC 31 October (Fig. 13). A total of 34.5-mm liquid-equivalent precipitation was melted down from the 25.9-cm measured snow (an SLR of about 7.5:1). The relatively low SLR implied that most of the snow would be heavily rimed, which agreed with the observations. The surface wind direction annotated on Fig. 13 showed a continuous west or northwest component (favored upslope for Poga Mountain) for at least a 72-h period, while wind speed (not shown) was slowly increasing throughout the event

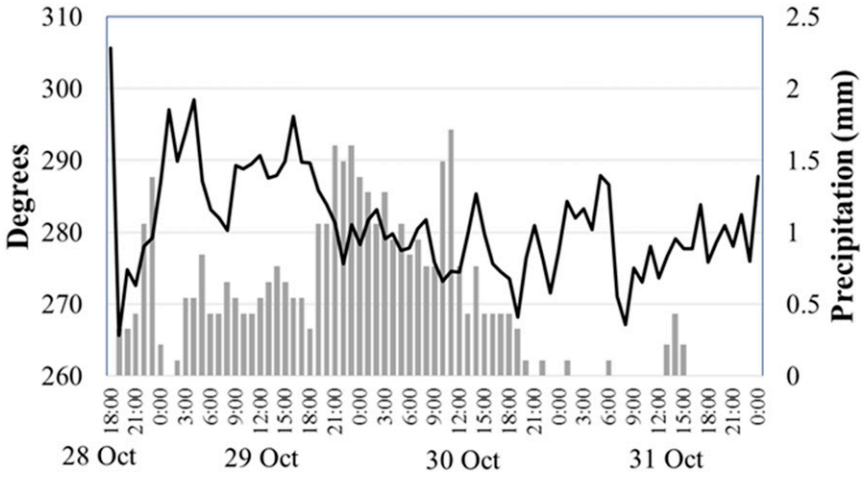

FIG. 13. Hourly liquid equivalent precipitation recorded at Poga Mountain (vertical bars) for the period 1800 UTC 28 Oct–0000 UTC 1 Nov 2012 (a correction for gauge undercatch is factored in based on total liquid equivalent measured manually), with average hourly surface wind direction also plotted.

even after the transition to lighter snow. Therefore, no obvious correlation appeared between surface wind and the change to lower snowfall rates.

c. *Contrast with a classic NWFS event*

An understanding of the uniqueness of the NWFS generated by Sandy can be placed into context by comparing its evolution with a case study considered to be a more typical or ''classic'' NWFS event. Observations of winter precipitation events made at Poga Mountain provide some of the basis for comparison between the conditions associated with the remnants of Sandy and the classic NWFS event of 26–28 February 2008. A simple comparison between the final snow accumulation for the Sandy event (Fig. 2) and the February 2008 NWFS event (Fig. 6) shows a much more significant snowfall with Sandy across the SAMs, yet a similar pattern in terms of the terrain signal with western slopes being favored.

In contrast to the synoptic conditions associated with Sandy (Figs. 9–11), the February 2008 NWFS event was associated with the movement of arctic air into the eastern United States with a high-amplitude upper-level trough (Fig. 14). The center of the parent cyclone was located far from the SAMs, and its position relative to a north–south-oriented building surface high pressure system aligned over the central United States generated a favorable pressure gradient, giving a prolonged 44-h period of upslope flow. An examination of 700-hPa-level vertical velocity and 750-hPa frontogenesis fields for the February 2008 event (Fig. 14b) reveals patterns qualitatively similar to those of the remnants of Sandy: strong signatures located over the SAMs confined to the lower troposphere (850–700-hPa layer), suggesting the presence of a mountain wave.

The Poga Mountain hourly precipitation rates and wind directions for the 26–28 February 2008 event (Fig. 15) show an overall shorter-duration event, yet the rates for at least a brief period of time were comparable with Sandy. Of note is that the snow accumulation dropped off by 1600 UTC (late morning) and then picked back up by late afternoon and into the evening. This is a common diurnal evolution that will be discussed more in section 5, but is not observed with Sandy (Fig. 13). Wind directions throughout this event, as with Sandy, were fairly steady from the west-northwest (tending a little more northwest compared to Sandy).

A vertically pointing Micro Rain Radar (MRR; Peters et al. 2002), in place on Poga Mountain during both NWFS events (Figs. 16 and 17), yielded time series of hydrometeor reflectivity (Figs. 16a and 17a) and fall velocities (Figs. 16b and 17b). Cloud tops during the time of maturation for the remnants of Sandy (Fig. 16a) reached nearly 3 km MSL, while the cloud tops at maturation for the classic NWFS event in February 2008 (Fig. 17a) were significantly shallower. The difference reflected the greater depth of the low-level moisture observed during Sandy's passage compared with typical NWFS events, when arctic air was passing through the SAMs. A more thorough discussion of moisture characteristics and comparisons with NWFS climatology follows in section 4.

Fall velocities as measured by the MRR at Poga Mountain were consistently greater for the remnants of Sandy (Fig. 16b) than for the classic February 2008 NWFS event (Fig. 17b). The fall velocity associated with

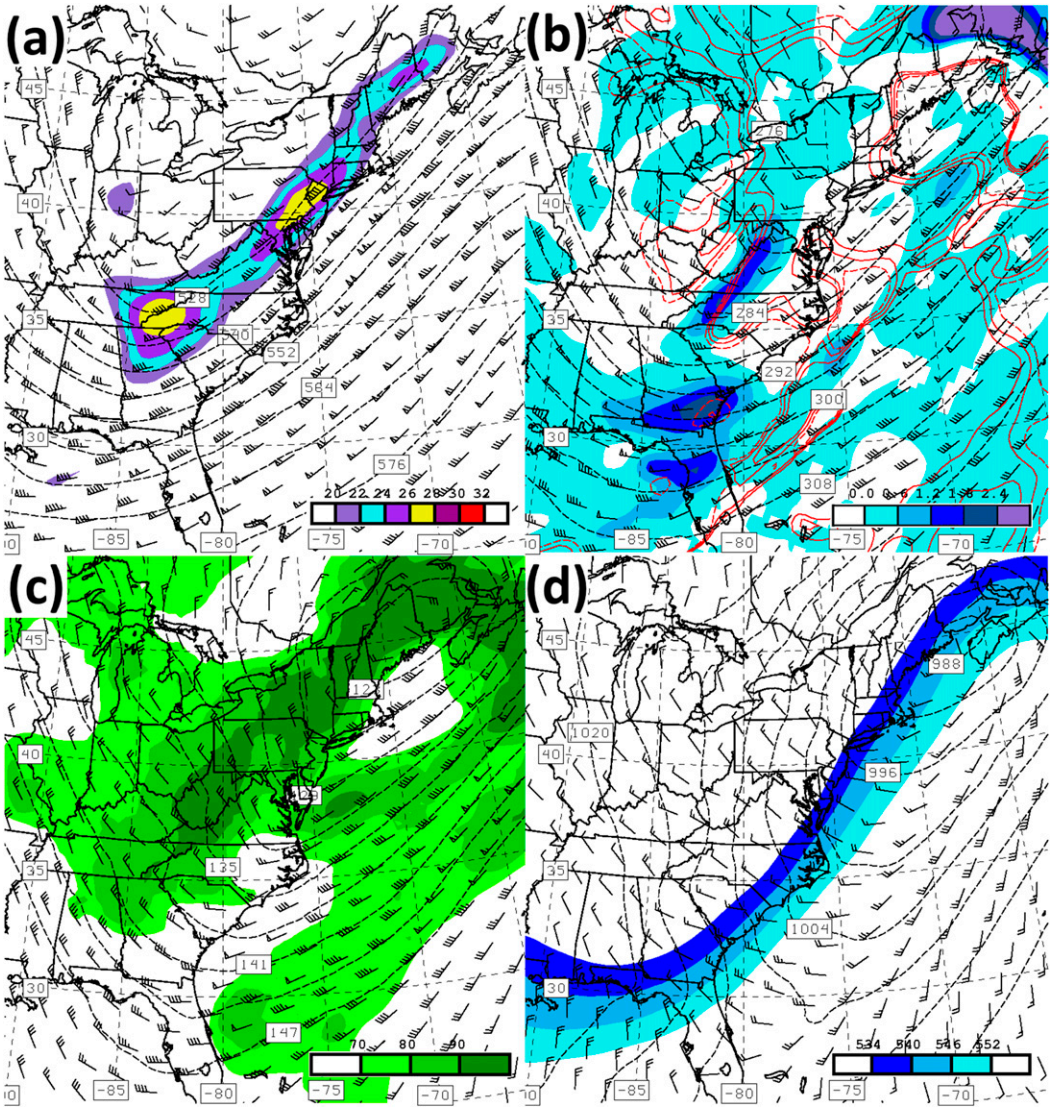

FIG. 14. As in Fig. 9, but for 1200 UTC 27 Feb 2008.

the increase in reflectivity centered around 1000 UTC 30 October (Fig. 16) showed a transition from values less than 2 m s^{-1} above 2 km MSL to values between 2 and 4 m s^{-1} below this level, perhaps because of ice crystals growing through riming and accretion as they fell through the very moist and cold layer closer to the ground. Fall velocity differences reflected differences in the observed habits of ice particles associated with each event: heavily rimed snow pellets of Sandy (mentioned previously) compared with unrimed dendritic crystals of the February 2008 event.

Table 1 provides a simple summary of the observations at Poga Mountain during the two events for easy comparison, and indicates the high liquid water content of the snow during passage of the remnants of Sandy compared to the more classic NWFS event. Examining a Rapid Refresh (RAP) model [formerly RUC; Benjamin et al. (2004, 2007)] initial analysis sounding at Poga Mountain valid at 0000 UTC 30 October (Fig. 18), when relatively high snowfall rates were observed during Sandy, indicates a shallow surface-based saturated layer but a subsaturated layer above that through at least around −20°C. This can be contrasted with the observed sounding during the 2008 February NWFS event shown earlier (Fig. 4), where the moisture is relatively shallow but the saturated layer is cold enough to suggest dendritic ice crystal growth. While the average observed surface wind speeds are similar between the two events, the soundings show that winds just above the surface at these two key times for each event were much stronger

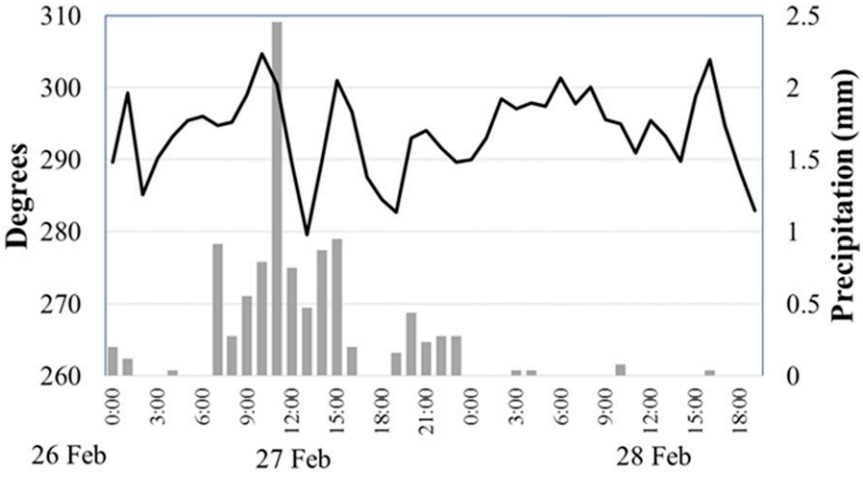

FIG. 15. As in Fig. 13, but for the period 0000 UTC 27 Feb–1800 UTC 28 Feb 2008.

with Sandy. A more thorough discussion of moisture characteristics follows in the next section.

4. Moisture characteristics and trajectory analysis

As mentioned earlier, much of the previous research on NWFS (Perry 2006; Perry et al. 2007; Holloway 2007) focused on synoptic climatology, upstream trajectories, and the influence of the Great Lakes connection (GLC). Some of this work specifically documented typical low-level moisture content along with near-ridgetop wind direction and speed for heavy versus light NWFS events. This section of the study will more closely examine the moisture characteristics and moisture sources associated

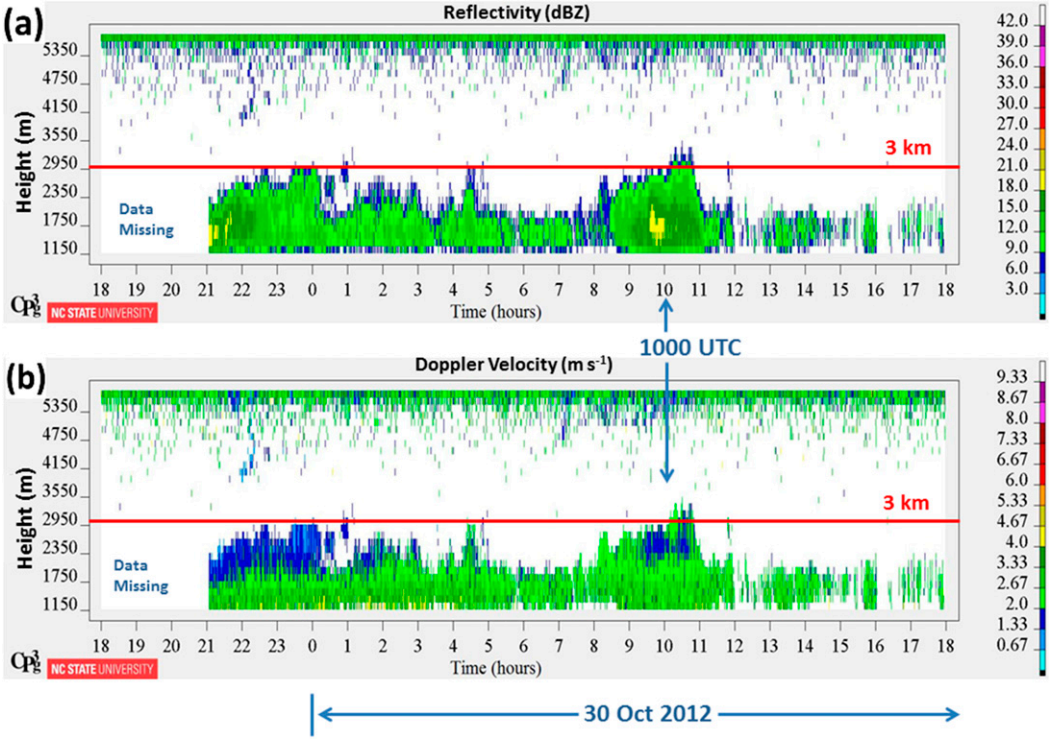

FIG. 16. Time series of (a) reflectivity (dBZ) and (b) Doppler velocity (m s^{-1}) from the vertically pointing MRR at Poga Mountain. Time advances from left to right (1800 UTC 29 Oct–1800 UTC 30 Oct 2012). Data are missing between 1800 and 2100 UTC on 29 Oct. Horizontal red line indicates 3 km MSL, and vertical blue arrows indicate the middle of an observed 6-h period of most intense snowfall at Poga Mountain.

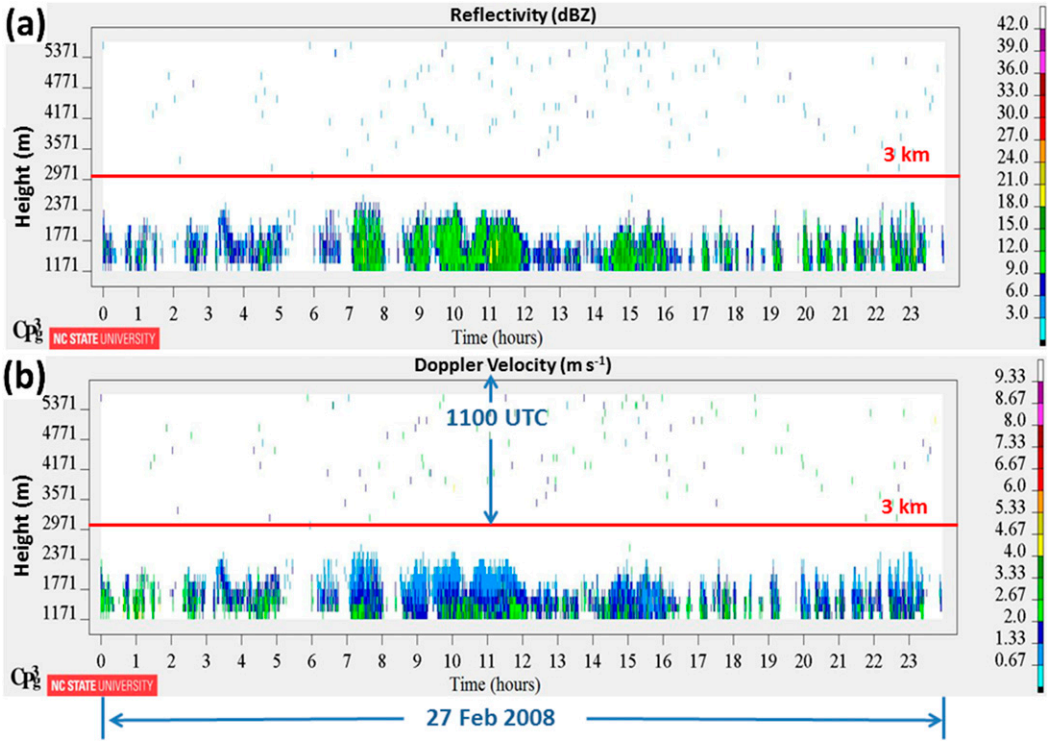

FIG. 17. As in Fig. 16, but for 0000–2359 UTC 27 Feb 2008.

with the Sandy snowfall event, as well as some low-level wind characteristics, and how these compare with the NWFS climatology examined in previous work.

a. *Data collection and methods*

Perry et al. (2007) produced a synoptic climatology from 432 NWFS events, divided these into "heavy" and "light" events, and evaluated a variety of synoptic fields for different geographic regions within the SAMs area, including one for elevations >1219 m, or "high peaks" [see Perry et al. (2007) for more details on how these categories and regions are defined]. To make comparisons between the Sandy snowfall event and the Perry et al. (2007) synoptic climatology of NWFS, data were collected for four high-elevation locations within the high-peaks region, which included High Knob, Virginia; Poga Mountain; Roan Mountain, Tennessee; and Mount LeConte, Tennessee (see Fig. 5 for these locations and their elevations). Because observed soundings do not exist across these higher elevations, the RAP model with a horizontal grid spacing of 13 km was used to construct soundings from the initial hour forecast (analysis). It is worth noting that the above-mentioned climatology developed by Perry et al. (2007) was based on finer-resolution reanalysis data from NCEP/NCAR and covered a geographic region, rather than for a few specific points from a coarser-resolution model. Several moisture and wind-related variables were retrieved from these four model sounding locations during Sandy snowfall, and are then compared to the Perry et al. (2007) NWFS climatology in Table 2.

b. *Moisture and wind characteristics*

The comparisons of several moisture and wind fields between Sandy and the Perry et al. (2007) NWFS climatology reveal generally much higher values

TABLE 1. Comparison of event total or average over the duration of the event for the remnants of Sandy (65-h duration, 0000 UTC 29 Oct–1700 UTC 31 Oct 2012) and of the classic NWFS event of February 2008 (44-h duration, 2300 UTC 26 Feb–1900 UTC 28 Feb 2008) as observed at Poga Mountain.

Event	Total snow (cm)	Total SWE (mm)	SLR	Mean temp (°C)	Mean RH (%)	Mean wind speed ($m\,s^{-1}$)	Mean wind direction (°)
Sandy	25.9	34.5	7.5	−2.44	97	5.4	273
Feb 2008	21.1	9.9	21.3	−7.18	91	5.3	295

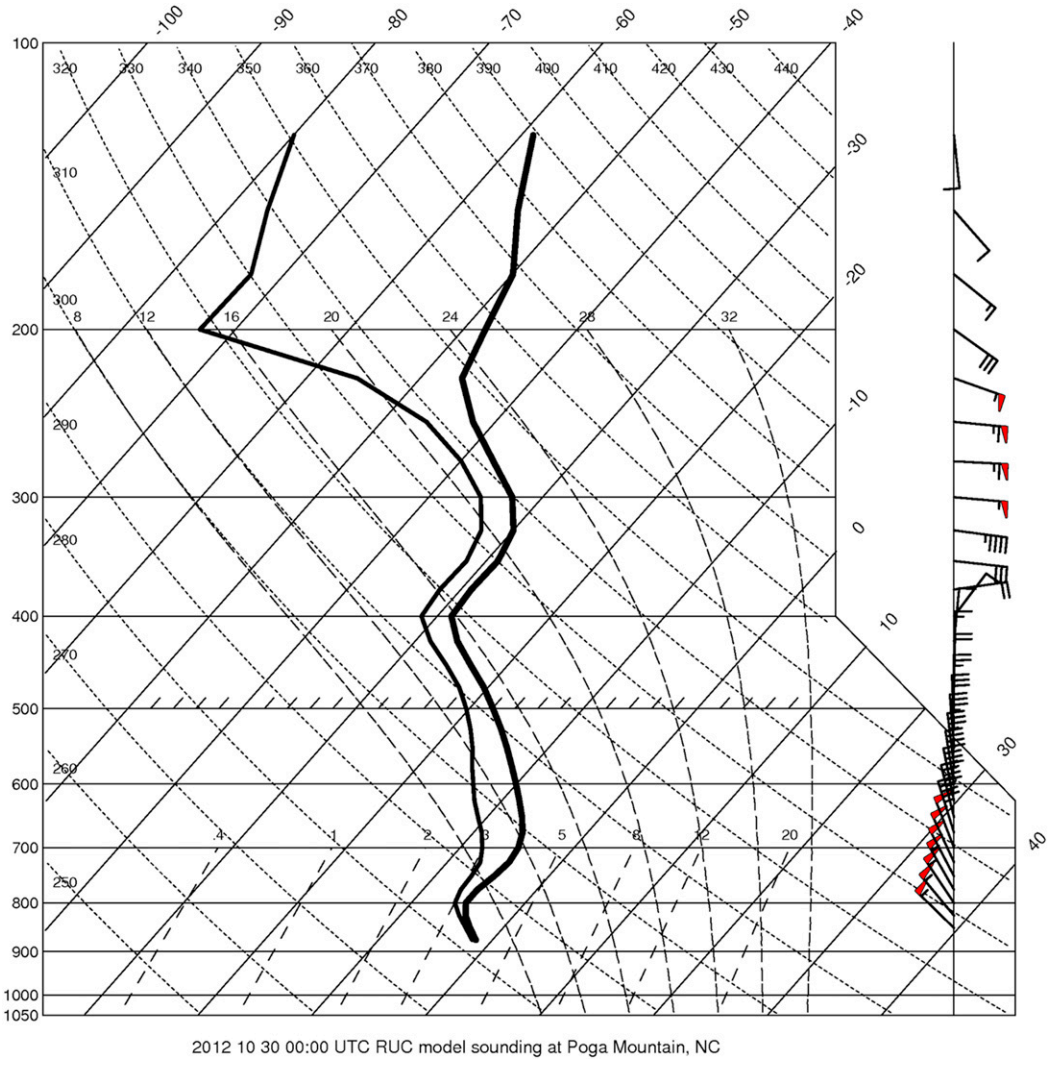

FIG. 18. Skew *T*–log*p* diagram of RAP model initial analysis profiles of temperature and dewpoint at Poga Mountain valid at 0000 UTC 30 Oct 2012.

associated with Sandy, as seen in Table 2. The four stations in Table 2 are organized from northernmost (top) to southernmost (bottom), and at the very bottom in boldface is a Sandy average of all of four stations along with the NWFS climatology for easy comparison.

An examination of precipitable water (PW) during Sandy at the four sites showed the values were higher than the NWFS high-peaks climatology for even the heavy snow cases. The thickness of the moist layer was also compared between Sandy and the NWFS climatology for these same high-peaks locations. A layer was determined to be moist if the relative humidity value was 80% or higher (as in Perry et al. 2007). Table 2 shows that the thickness of the moist layer during Sandy on average was much deeper than typical NWFS events, although the shallowest thicknesses (the latter stages of Sandy) were comparable to or even a little less than the values in the light NWFS climatology.

Perry et al. (2007) considered 850 hPa as the most appropriate level to examine moisture content and winds on the upstream side of the Appalachians because the orographic influence from these particular mountain ridges (ranging from 1000 to 2000 m) most closely matches this level compared to other standard levels. During the Sandy snowfall, the 850-hPa mixing ratio was also atypically high compared to the NWFS climatology (Table 2), contributing to the heavy snow and low SLRs as mentioned previously. NWFS climatology for the heavy 850-hPa mixing ratio average is 2.90 g kg^{-1}, but during Sandy even the average low mixing ratio was higher than this (3.10 g kg^{-1}).

TABLE 2. Comparison of total PW, thickness of moist layer, 850-hPa mixing ratio w, and 850-hPa wind speed during the Sandy snow event (max and min values observed at each site during the event) compared to typical values for high-peaks NWFS climatology of light and heavy events from Perry et al. (2007). An average from the four locations for the Sandy high, and also the Sandy low, is calculated at the bottom in boldface and again compared with the high-peaks NWFS climatology.

Location	Parameter	PW (mm)	Moist-layer depth (hPa)	850-hPa w (g kg^{-1})	850-hPa wind speed (m s^{-1})
High Knob	Sandy high	16.26	611	3.6	24.2
	Sandy low	12.70	256	3.1	15.4
	Climatology heavy	11.18	301	2.90	10.4
	Climatology light	10.67	203	2.84	9.3
Poga Mountain	Sandy high	15.49	566	3.7	27.8
	Sandy low	10.92	122	3.2	14.4
	Climatology heavy	11.18	301	2.90	10.4
	Climatology light	10.67	203	2.84	9.3
Roan Mountain	Sandy high	14.99	547	3.6	25.7
	Sandy low	12.19	157	3.1	13.9
	Climatology heavy	11.18	301	2.90	10.4
	Climatology light	10.67	203	2.84	9.3
Mount LeConte	Sandy high	14.22	502	3.7	22.6
	Sandy low	11.43	155	3.0	13.4
	Climatology heavy	11.18	301	2.90	10.4
	Climatology light	10.67	203	2.84	9.3
Sandy avg	**Sandy high**	**15.24**	**557**	**3.65**	**25.1**
	Sandy low	**11.81**	**173**	**3.10**	**14.3**
	Climatology heavy	**11.18**	**301**	**2.90**	**10.4**
	Climatology light	**10.67**	**203**	**2.84**	**9.3**

Meanwhile, the 850-hPa winds were between 20 and 26 m s^{-1} across most of the SAMs during the Sandy snowfall (refer to Figs. 9c and 10c). This strong northwest flow continued from the late evening on 29 October through early on 31 October. As seen in Table 2, the NWFS heavy climatology for 850-hPa winds averages 10.4 m s^{-1}, but during Sandy the average low 850-hPa wind speed was 14.3 m s^{-1} while the average high speed was 25.1 m s^{-1}. Considering the wind directions at this level had a significant orthogonal component to the ridges throughout the duration of Sandy as shown in section 3, this is further evidence that orographic lift was a dominant factor throughout most of the Sandy snowfall event—certainly stronger than typical NWFS events given the difference in observed 850-hPa wind speeds.

c. *Trajectory analysis of the Sandy snowstorm*

Previous NWFS research (Perry 2006; Perry et al. 2007; Holloway 2007) also looked at the contribution of the Great Lakes during snowfall events and showed that events having a GLC tended to produce higher snowfall totals compared to those having no GLC. In addition, Perry et al. (2007) found that almost half (47.1%) of the NWFS events within their study area of the SAMs had a GLC within a 72-h backward trajectory period and ending at event maturation, while only 10% had a low-level trajectory from the northeast United States or the mid-Atlantic area. For the Sandy snow event, backward trajectories from the HYSPLIT model (Draxler and Rolph 2014) were created for Mount LeConte and Snowshoe (points A and D, respectively, in Fig. 5), using the 40-km Eta Data Assimilation System (EDAS) archived initial analysis grids.

At 1000 UTC 30 October 2012, when some of the heaviest snowfall rates were occurring in western North Carolina, as shown in section 3, the HYSPLIT backward trajectories at 850 hPa (red lines) show a GLC at both locations (Fig. 19), although in the case of Snowshoe (Fig. 19b) that parcel was not near the surface when passing over the Great Lakes. In addition, the backward trajectories at both 700 hPa (blue lines) and 500 hPa (green lines) at both locations indicated flow across the Atlantic. While this evidence does not prove that there was any direct moisture flux from the ocean, the parcels arriving at Snowshoe at 500 and 700 hPa (Fig. 19b) more than likely passed through the deeper moisture associated with Sandy. Indeed, the 500-hPa parcel originated from near the surface while over the Atlantic, with high moisture content at that time. These parcels are also seen to rise significantly (especially the 700-hPa trajectory in Fig. 19b) as they came in over land and then approached from the north before arriving at Snowshoe. The rises in all three parcels immediately prior to arrival at Snowshoe confirm deeper lift at that location at this stage of the event. The traces at Mount LeConte at this time indicated a much greater likelihood of the Great Lakes being an important moisture source, and also that

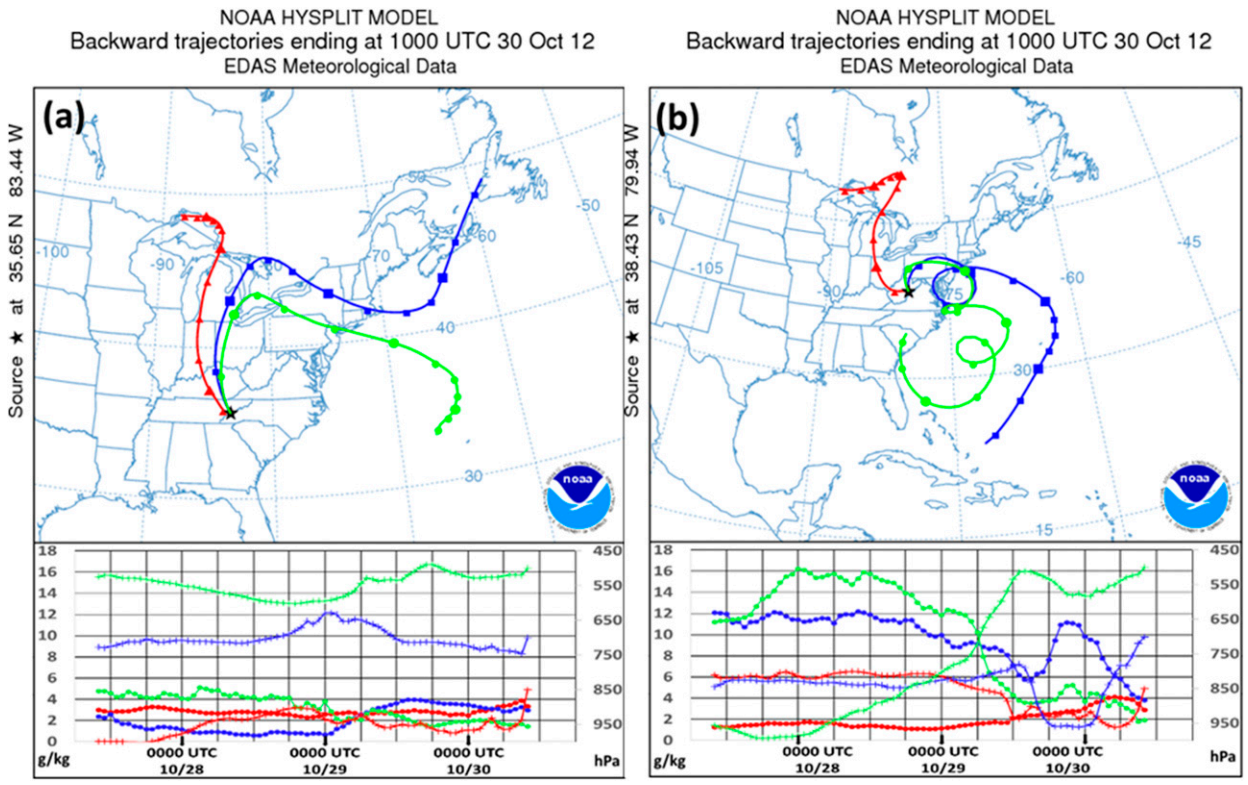

FIG. 19. Model-simulated backward trajectories from HYSPLIT for the 72-h period ending 1000 UTC 30 Oct 2012 at three levels ending at specified heights as indicated in the bottom portion of each image (500 hPa, green plus signs; 700 hPa, blue plus signs; 850 hPa, red plus signs). Mixing ratio (g kg^{-1}) values for each parcel are also overlaid with the pressure traces with the corresponding color, and traced with small filled circles. The grids for plots at the bottom of the panels correspond to the time steps shown in the plan-view trajectories at the top, where every 24-h increment (0000 UTC) is shown by a larger symbol. Shown are results for (a) Mount LeConte and (b) Snowshoe.

only the parcel arriving at 850 hPa experienced significant ascent immediately upon arrival.

Near the end of the Sandy snowstorm at 1700 UTC 31 October 2012, the HYSPLIT backward trajectories at 850 hPa (red lines) suggest that the GLC at both locations was diminishing, perhaps more so at Mount LeConte (Fig. 20a) compared to Snowshoe (Fig. 20b). Also, the midlevel flow over the Atlantic remained at Snowshoe with gradual ascent in the 700-hPa parcel as well as evidence that at one point this parcel was near the surface over the Atlantic (Fig. 20b), yet at Mount LeConte at this time (Fig. 20a) any flow from over the Atlantic appeared to have ended, with general subsidence for the 700- and 500-hPa parcels until just before arrival. The 850-hPa parcels for both locations remained near the surface the entire time but can be seen lifting up the western slopes just before arrival at both locations. These pressure plots again help confirm that at this time the vertical motion was much stronger in the lowest levels at both locations.

These trajectory analyses suggest that moisture associated with the heart of the Sandy circulation, and perhaps even direct Atlantic moisture, were important contributors in producing deeper and greater overall moisture content at Snowshoe, but made a limited contribution farther south at Mount LeConte. They also suggest that throughout the duration of the Sandy snowfall the influence of the Great Lakes on low-level air parcels arriving on the west-to-northwest-facing slopes of the SAMs appeared to be less than in some NWFS events. Despite a potentially more limited GLC, it can be argued that given the time of year the relatively warm Great Lakes temperatures and upstream ground temperatures may still have had a significant influence on boundary layer moisture and stability advected into the SAMs.

Finally, the trajectory analyses help to corroborate the evidence shown in section 3 for dominant orographic lift for most of the event but also offer evidence of some deeper ascent in the northern part of the study area during the first half. If the southern part of the area (i.e., Mount LeConte, Roan Mountain) experienced shallower lift and less moisture directly from the Atlantic compared to the northern part, this did not affect the

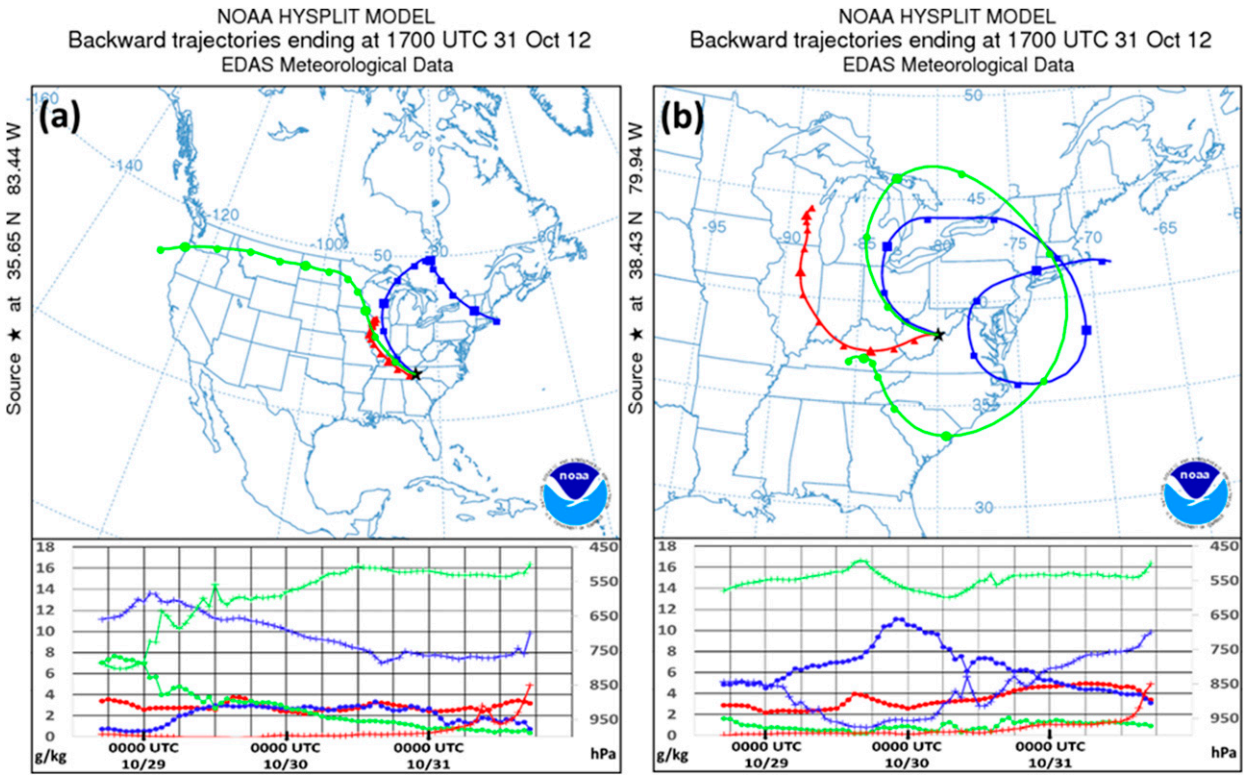

FIG. 20. As in Fig. 19, but for 1700 UTC 31 Oct 2012.

final snowfall totals at these locations compared to Snowshoe (Fig. 2). Elevation and immediate upstream relief is likely a significant factor in that this produced even greater upslope lift.

5. Radar observations and implications

a. Radar evidence of mountain wave activity

Strong northwesterly flow during the passage of the remnants of Sandy and the presence of a stable layer just above mountaintop level in western North Carolina (Fig. 18) created favorable conditions for the formation of mountain waves over and to the lee of the SAMs (Lindsay 1962) by the early evening of 29 October. NARR-based evidence of mountain wave formation was shown earlier in section 3. Here, a RAP model analysis at 0000 UTC 30 October for a vertical cross section for the same segment as in Fig. 12 (centered on Poga Mountain and orientated as line X–Y in Fig. 5) showed the classic signature of mountain waves (Fig. 21), as depicted by saturated equivalent potential temperature as well as relative humidity. Of note was the relatively high humidity through the depth of the inferred upward-directed air current in the mountain wave to the lee of the mountain ridge. At this time (specifically 0002 UTC 30 October), the Knoxville/Tri-Cities, Tennessee (KMRX) Weather Surveillance Radar-1988 Doppler (WSR-88D; Fig. 22) detected quasi-linear features in the base reflectivity on the lowest three elevation scans, oriented parallel to the mountain chain and tilted in the upstream direction with height (note the relative positions of line segments B–B′, C–C′, and D–D′ in Fig. 22). This feature remained anchored for several hours. The intersection of the linear reflectivity features with this region of upward vertical motion and high humidity (shown as points B and C in Fig. 21) suggested the development of hydrometeors large enough to be detected by the KMRX radar within the mountain wave.

The detection of the wave feature by radar was significant because it was direct evidence of the mechanical forcing provided by the strong northwesterly upslope flow at low- to midlevels and the relatively deep moisture available. It remains unclear whether or not the deep rearward-sloping upward vertical motion associated with the mountain wave played any role in the heavy snowfall rates on the immediate upstream side of the ridges. In more typical NWFS events the moisture was not this deep, although mountain waves likely occurred in many of them (as inferred by Fig. 14b).

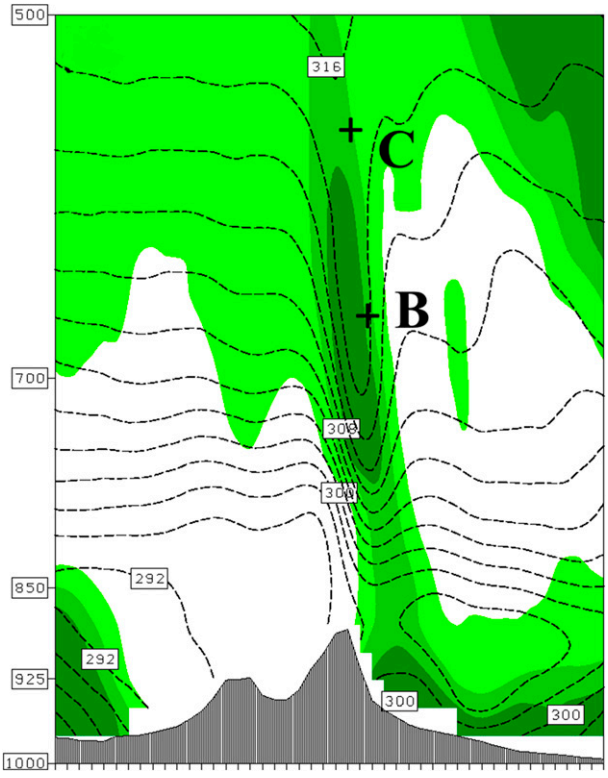

FIG. 21. Vertical cross section as analyzed by the RAP model at 0000 UTC 30 Oct 2012, depicting saturation equivalent potential temperature (dashed contours, 2-K intervals) and relative humidity (70%, 80%, and 90%; shaded). Points labeled B and C correspond to the height of the reflectivity band identified as a mountain wave (lines B–B′ and C–C′) in Fig. 22. Section is defined as line X–Y shown in Fig. 5 and is the same segment as in Fig. 12.

b. *Radar echo organization and low-level stability*

As mentioned previously, studies of other NWFS events (e.g., Holloway 2007) have determined that the Great Lakes are a potentially important moisture source at low levels and can act to destabilize the boundary layer. As the remnant circulation of Sandy turned northward on the morning of 30 October and the high clouds thinned, a plume of cloudiness and moisture was revealed in the infrared imagery curving southeastward from the vicinity of Lake Michigan toward northwest North Carolina (Fig. 23a). The RAP initial hour analysis at 1700 UTC 30 October showed a channel of surface-based convective available potential energy [CAPE; on the order of 25–50 J kg^{-1}, similar to CAPE ranges observed on the leeward shore during lake-effect snowstorms; cf. Fig. 4.22 of Markowski and Richardson (2010)] that also stretched from Lake Michigan to the northern mountains of North Carolina (Fig. 23c). The lapse rate in the boundary layer (0–1 km AGL) was in the 6.5°–8.5°C km^{-1} range within the CAPE channel (Fig. 23d), which was not as unstable as typical NWFS cases where precipitation banding occurred when boundary layer lapse rates exceeded 9°C km^{-1} (e.g., Fig. 4). Wind streamlines in the 0–1-km layer also showed the flow moving down the long axis of Lake Michigan and curving southeasterly toward northwest North Carolina (Fig. 23b). The band of CAPE and a relatively weak boundary layer lapse rate persisted from 1500 to about 2300 UTC 30 October.

At this same time (1700 UTC 30 October), a large mass of light precipitation was observed over northeast Tennessee and eastern Kentucky with a stratiform appearance (Fig. 24a), while visible satellite imagery (Fig. 24b) showed a dense overcast curving down from the northwest and likely extending all the way back toward the Great Lakes based on the infrared image in Fig. 23a. In spite of the low-level GLC and the trajectory of air parcels across a region with weak surface-based buoyancy, the precipitation failed to organize into cells and bands as observed in other NWFS events in the presence of weak CAPE during daylight hours (e.g., Hudgins 2008). In contrast to Sandy, the precipitation elements in the 27 February 2008 NWFS case became loosely organized into cells and bands during the time of peak heating (Fig. 24c), while satellite imagery also gave the appearance of open-cell convection over northeast Tennessee (Fig. 24d). The weaker boundary layer lapse rates in the Sandy event, perhaps brought about by the dense cloud cover, may have inhibited the development of convective elements during the afternoon of 30 October. The diurnal evolution toward more convective elements in typical NWFS events often limits the daytime accumulations of snowfall to some extent (Miller 2012), whereas with Sandy a somewhat steadier snowfall rate was still observed at some of the higher-elevation locations during the day on 30 October (i.e., Roan Mountain where about 10 cm of additional accumulation occurred; not shown). Awareness of factors that can modulate boundary layer stability and thus influence the diurnal behavior of snowfall rates in NWFS events may lead to improved short-term forecasts.

6. Conclusions

The remnants of Hurricane Sandy had a historic impact on much of the eastern United States, including a significant early season NWFS for the SAMs, which heretofore has received little attention in the literature compared to the coastal impacts of the storm. Given the extreme paucity of tropical systems that result in snowfall over the eastern United States, it was not surprising that Sandy did not fit into any of the previously

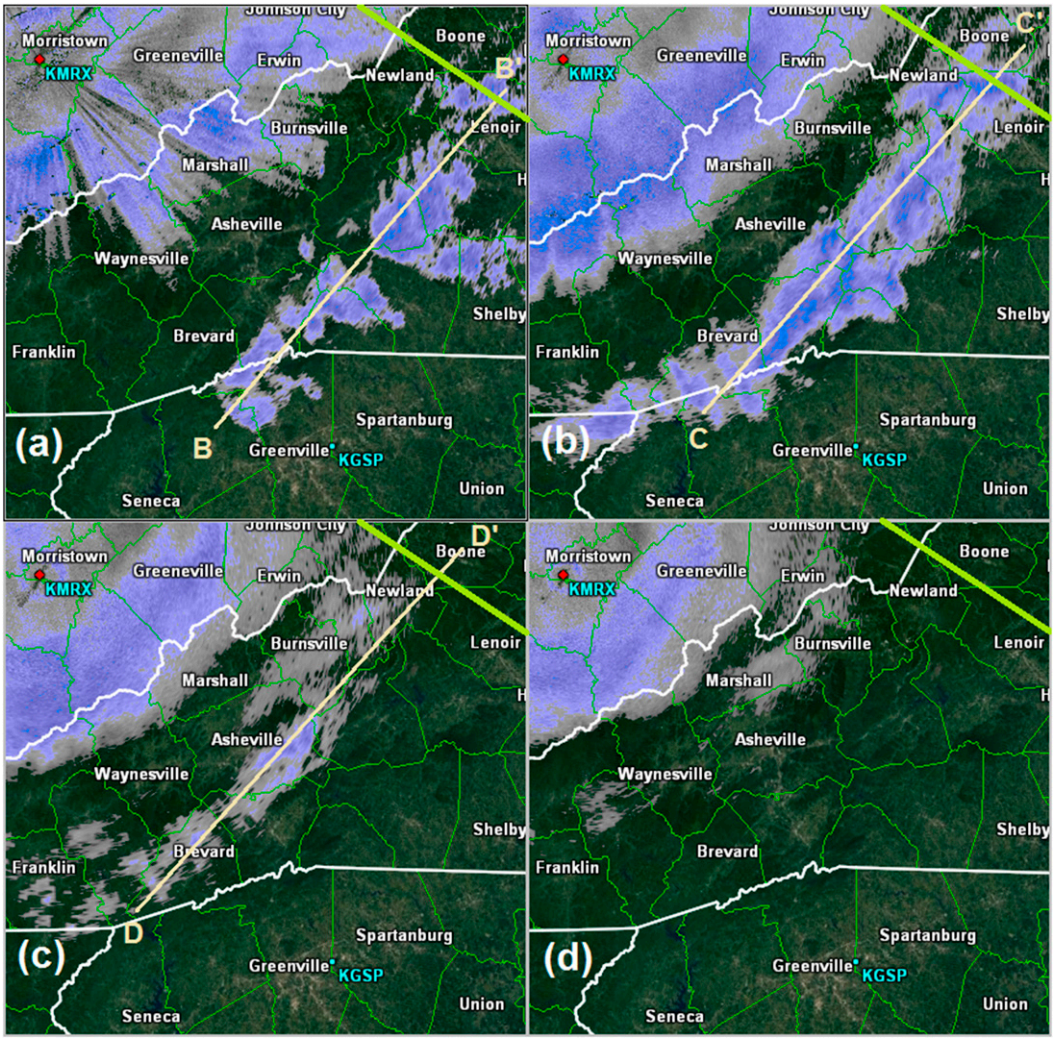

FIG. 22. Base reflectivity from the KMRX radar at 0002 UTC 30 Oct 2012 on the (a) 0.5°, (b) 1.5°, (c) 2.4°, and (d) 3.4° scans. The green line denotes the location of the vertical cross section in Fig. 5. The lines B–B′, C–C′, and D–D′ correspond to the mountain wave signature at that elevation. The intersections of lines B–B′ and C–C′ with the vertical cross section are shown as points B and C in Fig. 21.

documented synoptic classes typically associated with the onset of NWFS in the SAMs. The rare synoptic setting with a hurricane transitioning to an extratropical system while interacting with a negatively tilted midlatitude system, thus turning northwest and slowing down, contributed to the duration and intensity of the northwest flow as well as the anomalous moisture content and depth. These were all significant factors in terms of final snow amounts, as well as the amount of drifting.

The analysis of forcing mechanisms suggested some degree of spatial and temporal complexity across the study area, with evidence for a period of larger-scale and deeper lift farther north, while forcing across southern portions of the area was primarily influenced by the terrain. The analysis also suggested that overall the relatively shallow upslope lift was a dominant mechanism for precipitation production for a majority of the event and over most of the SAMs region. The transition from higher snowfall rates to lower rates observed at Poga Mountain (and also places like Roan Mountain) was more likely related to the depth of the moisture and, perhaps, to some degree to a decrease in ridgetop wind magnitude orthogonal to the ridge orientation, rather than any changes in the vertical motion depth or mechanisms.

Upstream backward trajectories also confirmed a connection to the Great Lakes, at least for a portion of the event. Given the season, the Great Lakes surface temperatures were warmer than for a typical NWFS

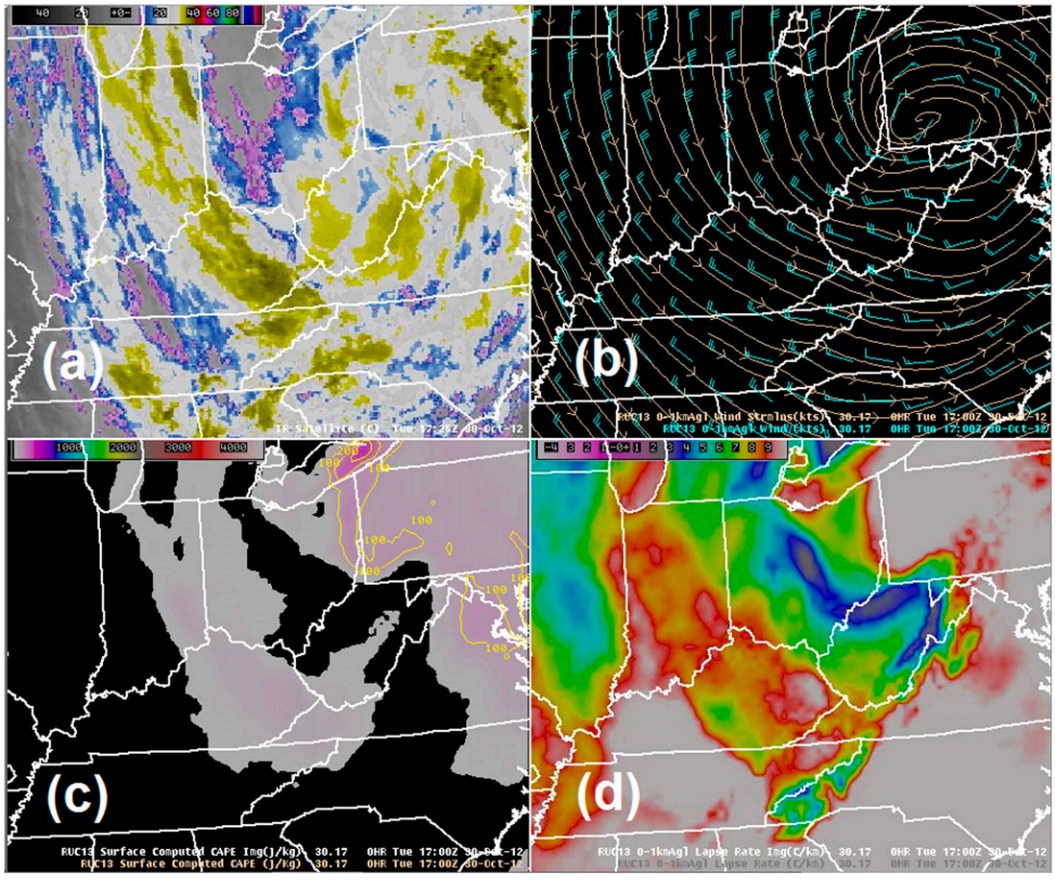

FIG. 23. (a) *GOES-13* satellite imagery in the IR window, along with RAP (labeled RUC13 on these images) initial analyses of (b) 0–1-km wind (kt) barbs and streamlines, (c) surface-based CAPE (J kg^{-1}; yellow contours and color filled), and (d) 0–1-km lapse rate (°C km^{-1}; color filled, red and white shades > 9°C km^{-1}) at 1700 UTC 30 Oct 2012.

event, which may have been an important contributing factor to boundary layer instability (albeit observed to be less than a typical NWFS event) and surface moisture flux. The trajectory analysis also showed evidence for at least the northern part of the region having a connection to moisture coming from the Atlantic and from near the center of Sandy's circulation when offshore.

Differences in boundary layer moisture and stability between Sandy and more typical NWFS events may have resulted in a departure from the more typical diurnal evolution of the convective nature observed with many NWFS events, as seen in observed precipitation rates as well as radar observations near the Tennessee–North Carolina border. This may have helped some light snow accumulations to last longer into the daytime hours during Sandy, even after the moisture became shallower toward the end. The unusually deep moisture content during the heart of the snowfall event likely also aided visualization of various radar phenomena discussed, such as the mountain wave, that are not as easily observed when moisture is extremely shallow and radars overshoot most of the precipitation growth layer.

More in-depth study of many of the aspects discussed above would answer some lingering research and operational questions. This is especially important given the review here is observationally based, and does not offer precise physical evidence as to the relative importance of the various factors described in this work. For example, numerical simulation reruns of this event could measure the contribution of Atlantic moisture, Great Lakes heat fluxes, and the strength of the wind speed on producing orographic lift and its relative importance compared to any apparently weaker synoptic lift during the early part of the event. Attempts to simulate the mountain waves highlighted in radar observations could provide insights into the potential contribution these may have made to the overall snow or wind impacts in the SAMs.

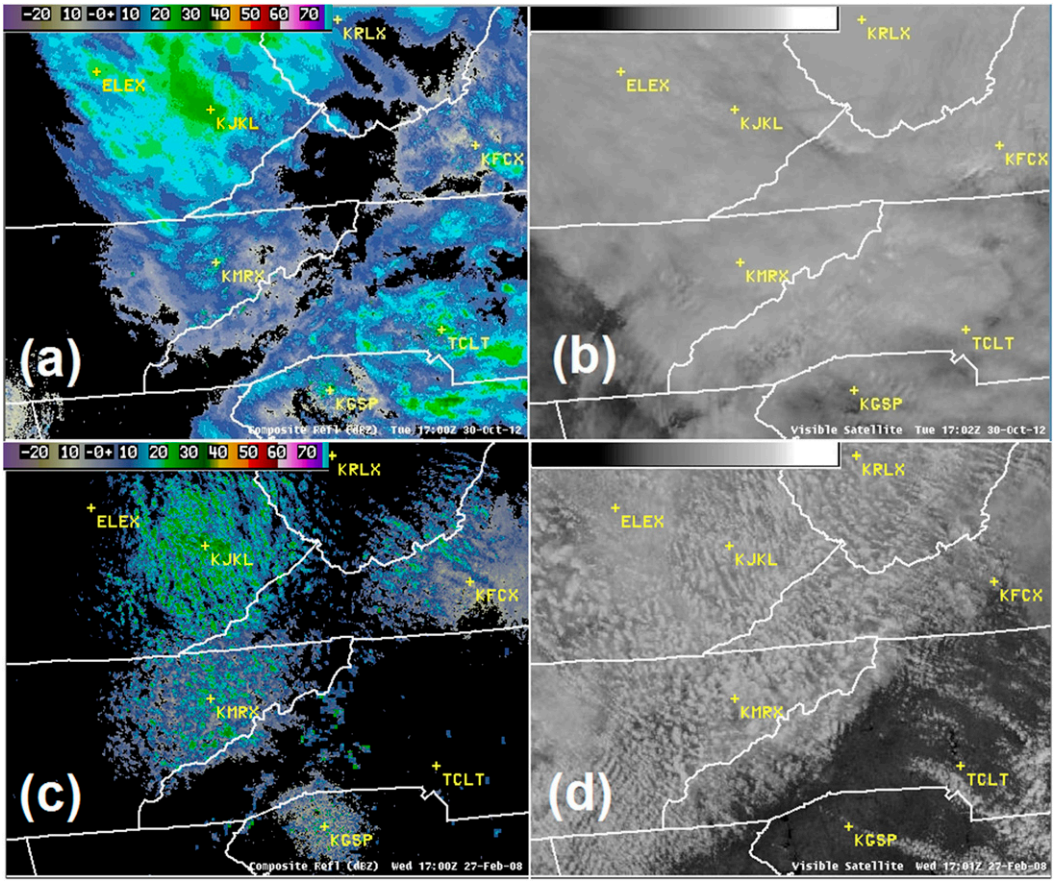

FIG. 24. (a) Composite reflectivity mosaic at 1700 UTC 30 Oct 2012 and (b) *GOES-13* visible satellite image at 1702 UTC 30 Oct 2012. For comparison, shown are (c) composite reflectivity mosaic at 1700 UTC 27 Feb 2008 and (d) *GOES-12* visible satellite image at 1701 UTC 27 Feb 2008.

Acknowledgments. The authors gratefully acknowledge S. Yuter for assistance with the visualization and analysis of the MRR imagery. In addition, Jason Endries helped with some of the figures for Poga Mountain snowfall rates. NWS cooperative observers, CoCoRaHS observers, law enforcement and emergency management officials, and the public provided snowfall reports that aided in the documentation of this event. The Roan Mountain observations are based upon work supported by the National Science Foundation under Grant EAR 0949263. We also appreciate the very helpful manuscript reviews from colleagues at the National Weather Service Eastern Region Headquarters, Scientific Services Division, as well as those of three anonymous formal reviewers, which all helped to significantly improve the paper. Reference to any specific commercial products, processes, or services by trade name, trademark, manufacturer, or otherwise, does not constitute or imply its recommendation, or favoring by the U.S. government, NOAA/National Weather Service, the state of North Carolina, Appalachian State University, or UNC Asheville. Use of information from this publication concerning proprietary products or tests of such products shall not be used for advertising or product endorsement purposes.

REFERENCES

Benjamin, S. G., and Coauthors, 2004: An hourly assimilation–forecast cycle: The RUC. *Mon. Wea. Rev.*, **132**, 495–518, doi:10.1175/1520-0493(2004)132<0495:AHACTR>2.0.CO;2.

——, and Coauthors, 2007: From the radar-enhanced RUC to the WRF-based Rapid Refresh. Preprints, *22nd Conf. Weather Analysis and Forecasting/18th Conf. on Numerical Weather Prediction*, Park City, UT, Amer. Meteor. Soc., J3.4. [Available online at https://ams.confex.com/ams/pdfpapers/124827.pdf.]

Blake, E. S., T. B. Kimberlain, R. J. Berg, J. P. Canglialosi, and J. L. Beven II, 2013: Tropical cyclone report – Hurricane Sandy (AL182012) 22–29 October 2012. National Hurricane Center, 157 pp. [Available online at http://www.nhc.noaa.gov/data/tcr/AL182012_Sandy.pdf.]

Department of Commerce, 1952: Climatological data: New England—February 1952. Vol. LXIV, No. 2, 20 pp.

Draxler, R. R., and G. D. Rolph, 2014: HYSPLIT - Hybrid Single-Particle Lagrangian Integrated Trajectory model. NOAA/Air Resources Laboratory, Silver Spring, MD. [Available online at http://ready.arl.noaa.gov/HYSPLIT.php.]

Dunn, G. E., 1964: The hurricane season of 1963. *Mon. Wea. Rev.*, **92**, 128–138, doi:10.1175/1520-0493-92.3.128.

FEMA, 2012: West Virginia–Hurricane Sandy. FEMA Preliminary Damage Assessment Rep. FEMA-4093-DR, 3 pp. [Available online at http://www.fema.gov/media-library-data/20130726-1901-25045-2859/dhs_ocfo_pda_report_fema_4093_dr_wv.pdf.]

Galarneau, T., C. Davis, and M. Shapiro, 2013: Intensification of Hurricane Sandy (2012) through extratropical warm core seclusion. *Mon. Wea. Rev.*, **141**, 4296–4321, doi:10.1175/MWR-D-13-00181.1.

Holloway, B. S., 2007: The role of the Great Lakes in northwest flow snowfall events in the southern Appalachian Mountains. M.S. thesis, Dept. of Marine, Earth, and Atmospheric Sciences, North Carolina State University, 204 pp. [Available online at http://www.lib.ncsu.edu/resolver/1840.16/1202.]

Hudgins, J., 2008: Mesoscale snowbands persisting downstream of the southern Appalachians during northwest flow upslope events. *33rd National Weather Association Annual Meeting*, Louisville, KY, National Weather Association, P3.4 [Available online at http://www.nwas.org/meetings/abstracts/display.php?id=306.]

Keighton, S., and L. G. Lee, 2013: Northwest flow snow aspects of Sandy. Part I: A general overview of NWFS in the southern Appalachians. *Extended Abstracts*, *38th National Weather Association Annual Meeting*, Charleston, SC, National Weather Association, 6.1. [Available online at http://www.nwas.org/meetings/nwa2013/extendedabstracts/NWA2013_SessionVI_Keighton_Lee.pdf.]

——, and Coauthors, 2009: A collaborative approach to study northwest flow snow in the southern Appalachians. *Bull. Amer. Meteor. Soc.*, **90**, 979–991, doi:10.1175/2009BAMS2591.1.

Libbrecht, K. G., 2005: The physics of snow crystals. *Rep. Prog. Phys.*, **68**, 855–895, doi:10.1088/0034-4885/68/4/R03.

Lindsay, C. V., 1962: Mountain waves in the Appalachians. *Mon. Wea. Rev.*, **90**, 271–276, doi:10.1175/1520-0493(1962)090<0271:MWITA>2.0.CO;2.

Ludlum, D. M., 1963: *Early American Hurricanes, 1492–1870.* Amer. Meteor. Soc., 212 pp.

Markowski, P., and Y. Richardson, 2010: *Mesoscale Meteorology in Midlatitudes*. Wiley-Blackwell, 407 pp.

Martin, D. T., 2013: Snowfall event characteristics from a high-elevation site in the southern Appalachian Mountains. M.A. thesis, Dept. of Geography and Planning, Appalachian State University, 69 pp. [Available online at http://www.int-res.com/abstracts/cr/v63/n3/p171-190/.]

Miller, D. K., 2012: Near-term effects of the lower atmosphere in simulated northwest flow snowfall forced over the southern Appalachians. *Wea. Forecasting*, **27**, 1198–1216, doi:10.1175/WAF-D-11-00103.1.

Niziol, T. A., W. R. Snyder, and J. S. Waldstreicher, 1995: Winter weather forecasting throughout the eastern United States. Part IV: Lake effect snow. *Wea. Forecasting*, **10**, 61–77, doi:10.1175/1520-0434(1995)010<0061:WWFTTE>2.0.CO;2.

Perry, L. B., 2006: Synoptic climatology of northwest flow snow in the southern Appalachians. Ph.D. dissertation, University of North Carolina at Chapel Hill, 176 pp.

——, and C. E. Konrad, 2006: Relationships between NW flow snowfall and topography in the southern Appalachians, USA. *Climate Res.*, **32**, 35–47, doi:10.3354/cr032035.

——, ——, and T. W. Schmidlin, 2007: Antecedent upstream air trajectories associated with northwest flow snowfall in the southern Appalachians. *Wea. Forecasting*, **22**, 334–352, doi:10.1175/WAF978.1.

——, D. K. Miller, S. E. Yuter, L. G. Lee, and S. J. Keighton, 2008: Atmospheric influences on new snow density in the southern Appalachian Mountains, USA. *Proc. 65th Eastern Snow Conf.*, Fairlee, VT, Eastern Snow Conference, 123–133. [Available online at http://www.easternsnow.org/proceedings/2008/perry_et_al.pdf.]

——, C. E. Konrad, D. Hotz, and L. G. Lee, 2010: Synoptic classification of snowfall events in the Great Smoky Mountains, USA. *Phys. Geogr.*, **31**, 156–171, doi:10.2747/0272-3646.31.2.156.

——, S. J. Keighton, L. G. Lee, D. K. Miller, S. E. Yuter, C. E. Konrad, and M. T. Bryant, 2013: Synoptic influences on snowfall event characteristics in the southern Appalachian mountains. *Proc. 70th Eastern Snow Conf.*, Huntsville, ON, Canada, Eastern Snow Conference, 141–157. [Available online at http://climate.appstate.edu/~perrylb/Pubs/Perry_etal_2013_ESC.pdf.]

Peters, G., B. Fischer, and T. Andersson, 2002: Rain observations with a vertically looking Micro Rain Radar (MRR). *Boreal Environ. Res.*, **7**, 353–362.

Schmidlin, T. W., 1992: Does lake-effect snow extend to the mountains of West Virginia? *Proc. 49th Eastern Snow Conf.*, Oswego, NY, Eastern Snow Conference, 145–148.

Strom, E., and R. Kerstein, 2015: Mountains and muses: Tourism development in Asheville, North Carolina. *Ann. Tourism Res.*, **52**, 134–147, doi:10.1016/j.annals.2015.03.006.